

# Multicomponent compact Abelian-Higgs lattice models

Andrea Pelissetto

*Dipartimento di Fisica dell'Università di Roma Sapienza and INFN Sezione di Roma I, I-00185 Roma, Italy*

Ettore Vicari

*Dipartimento di Fisica dell'Università di Pisa and INFN Largo Pontecorvo 3, I-56127 Pisa, Italy*

(Dated: December 25, 2021)

We investigate the phase diagram and critical behavior of three-dimensional multicomponent Abelian-Higgs models, in which an  $N$ -component complex field  $z_{\mathbf{x}}^a$  of unit length and charge is coupled to compact quantum electrodynamics in the usual Wilson lattice formulation. We determine the phase diagram and study the nature of the transition line for  $N = 2$  and  $N = 4$ . Two phases are identified, specified by the behavior of the gauge-invariant local composite operator  $Q_{\mathbf{x}}^{ab} = \bar{z}_{\mathbf{x}}^a z_{\mathbf{x}}^b - \delta^{ab}/N$ , which plays the role of order parameter. In one phase, we have  $\langle Q_{\mathbf{x}}^{ab} \rangle = 0$ , while in the other  $Q_{\mathbf{x}}^{ab}$  condenses. Gauge correlations are never critical: gauge excitations are massive for any finite coupling. The two phases are separated by a transition line. Our numerical data are consistent with the simple scenario in which the nature of the transition is independent of the gauge coupling. Therefore, for any finite positive value of the gauge coupling, we predict a continuous transition in the Heisenberg universality class for  $N = 2$  and a first-order transition for  $N = 4$ . However, notable crossover phenomena emerge for large gauge couplings, when gauge fluctuations are suppressed. Such crossover phenomena are related to the unstable  $O(2N)$  fixed point, describing the behavior of the model in the infinite gauge-coupling limit.

## I. INTRODUCTION

Models of complex scalar matter fields coupled to gauge fields have been much studied in condensed matter physics, since they are believed to describe several interesting systems, such as superconductors and superfluids, quantum Hall states, quantum  $SU(N)$  antiferromagnets, unconventional quantum phase transitions, etc., see, *e.g.*, Refs. [1–6] and references therein. Scalar electrodynamics, or Abelian-Higgs (AH) model, is a paradigmatic model, in which a  $N$ -component complex scalar field  $\Phi$  is minimally coupled to the electromagnetic field  $A_{\mu}$ . The corresponding continuum Lagrangian reads

$$\mathcal{L} = |D_{\mu}\Phi|^2 + r|\Phi|^2 + \frac{1}{6}u(|\Phi|^2)^2 + \frac{1}{4g^2}F_{\mu\nu}^2, \quad (1)$$

where  $F_{\mu\nu} \equiv \partial_{\mu}A_{\nu} - \partial_{\nu}A_{\mu}$ , and  $D_{\mu} \equiv \partial_{\mu} + iA_{\mu}$ . The renormalization-group (RG) analysis of the continuum AH model [7, 8] should provide information on the nature of the finite-temperature phase transitions occurring in  $d$ -dimensional systems characterized by a global  $U(N)$  symmetry and a local  $U(1)$  gauge symmetry.

In this paper we consider the multicomponent AH model, in which the scalar field  $\Phi$  has  $N \geq 2$  components. Such a model has a local  $U(1)$  gauge invariance and a global  $U(N)$  invariance. We assume that the field belongs to the fundamental representation of the  $U(1)$  group, *i.e.*, it has charge 1. The one-component AH model has been extensively discussed in the literature [9–13]. In three dimensions, these systems may undergo continuous transitions in the XY universality class.

Lattice formulations of the three-dimensional AH model are obtained by associating complex  $N$ -component unit vectors  $z_{\mathbf{x}}$  with the sites  $\mathbf{x}$  of a cubic lattice, and  $U(1)$  variables  $\lambda_{\mathbf{x},\mu}$  with each link connecting the site  $\mathbf{x}$

with  $\mathbf{x} + \hat{\mu}$  (where  $\hat{\mu} = \hat{1}, \hat{2}, \dots$  are unit vectors along the lattice directions). The partition function of the system reads

$$Z = \sum_{\{\mathbf{z}\}, \{\lambda\}} e^{-H}, \quad (2)$$

where the Hamiltonian is [14]

$$H = -\beta N \sum_{\mathbf{x}, \mu} (\bar{z}_{\mathbf{x}} \cdot \lambda_{\mathbf{x},\mu} z_{\mathbf{x}+\hat{\mu}} + \text{c.c.}) \quad (3) \\ - \beta_g \sum_{\mathbf{x}, \mu \neq \nu} (\lambda_{\mathbf{x},\mu} \lambda_{\mathbf{x}+\hat{\mu},\nu} \bar{\lambda}_{\mathbf{x}+\hat{\nu},\mu} \bar{\lambda}_{\mathbf{x},\nu} + \text{c.c.}),$$

where the first sum is over all links of the lattice, while the second one is over all plaquettes.

For  $\beta_g = 0$  we recover a particular lattice formulation of the  $CP^{N-1}$  model, which is quadratic with respect to the spin variables and contains explicit gauge link variables. The  $CP^{N-1}$  model has been extensively studied. In spite of several field-theoretical and numerical studies for  $N = 2, 3, 4$  and  $N \rightarrow \infty$ , there are still some controversies on the nature of its transition [6, 8, 15–19]. For  $\beta_g \rightarrow \infty$  the gauge link variables are all equal to 1 modulo gauge transformations and the AH model becomes equivalent to the standard  $O(n)$  vector model with  $n = 2N$ , whose critical behavior is well understood [20]. We also mention that some numerical results for the AH lattice model (3) have been reported in Refs. [6, 21, 22], but a definite picture has not been achieved yet [23].

It is important to stress that we consider the lattice compact version of electrodynamics (the so-called Wilson lattice formulation of gauge theories). In the absence of matter fields, its behavior [24] is controlled by topological excitations, the monopoles, which are instead suppressed in noncompact formulations. Therefore, the

critical properties of the AH lattice model that we consider might differ from those of the model in which gauge fields are noncompact.

In this paper we investigate the phase diagram and the nature of the phase transitions of the three-dimensional AH model (3). We consider systems with  $N = 2$  and  $N = 4$ , and investigate the nature of the transition line by varying  $\beta$  at fixed gauge coupling  $\beta_g$ , for some values of  $\beta_g$ . In both cases the phase diagram of the AH lattice model (3) turns out to present two phases: for small  $\beta$  there is a disordered confined phase, while for large values of  $\beta$  there is an ordered Higgs phase in which correlations of the gauge-invariant hermitian operator  $Q_{\mathbf{x}}^{ab} = \bar{z}_{\mathbf{x}}^a z_{\mathbf{x}}^b - \delta^{ab}/N$  show long-range order. In both phases, and also along the transition line, the correlations of gauge variables do not show critical behaviors. The gauge coupling  $\beta_g$  does not play any significant role: the features of two phases are the same for any finite  $\beta_g$ . The two phases are separated by a single transition line, which connects the  $\text{CP}^{N-1}$  transition point ( $\beta_g = 0$ ) to the  $\text{O}(2N)$  transition point ( $\beta_g = \infty$ ) in the space of the two parameters  $\beta$  and  $\beta_g$ . For  $\beta_g = 0$  the transition is continuous for  $N = 2$  (belonging to the Heisenberg universality class) and of first order for  $N = 4$ . We conjecture that the nature of the transitions along the line separating the Higgs and confined phases does not change with  $\beta_g$ . Therefore, the transition is always continuous (discontinuous) for  $N = 2$  ( $N = 4$ ). We also observe significant deviations for  $\beta_g$  large ( $\beta_g \gtrsim 1$ ), i.e., when gauge fluctuations are suppressed. They are interpreted as a crossover phenomenon due to the presence of a  $\text{O}(2N)$  vector transition in the limit  $\beta_g \rightarrow \infty$ .

The paper is organized as follows. In Sec. II we review the field-theoretical results for the AH model. In Sec. II A we review the  $\varepsilon$ -expansion predictions obtained in the continuum AH model, and in Sec. II B we present instead the results of the Landau-Ginzburg-Wilson (LGW) approach based on a gauge-invariant order parameter. The two approaches are critically compared in Sec. II C. The numerical results are presented in Sec. III. The definitions of the quantities we consider are given in Sec. III A, while Sec. III B and III C present our results for  $N = 2$  and 4, respectively, focusing on the behavior of the gauge-invariant order parameter. Results for vector and gauge observables are presented in Sec. III D. In Sec. IV we summarize and present our conclusions. In App. A we discuss the limit  $\beta_g \rightarrow \infty$ . More details on the behavior of the different observables in this limit are given in the supplementary material [25].

## II. FIELD THEORETICAL APPROACHES

In this section we outline some apparently alternative field-theoretical approaches which can be employed to infer the nature of the phase transitions in systems characterized by a  $\text{U}(N)$  global symmetry and a local  $\text{U}(1)$  gauge symmetry, such as the AH lattice model.

### A. Renormalization-group flow in the AH model close to four dimensions

We now summarize the main features of the RG flow in the continuum AH model (1), which has been analyzed close to four dimensions in the  $\varepsilon \equiv 4 - d$  expansion framework [7, 26, 27], and in the large- $N$  limit [8].

Close to four dimensions, the RG flow in the space of the renormalized couplings  $u$  and  $f \equiv g^2$  (we rescale them as  $u \rightarrow u/(24\pi^2)$  and  $f \rightarrow f/(24\pi^2)$  to simplify the equations) can be computed in perturbation theory. At one loop, the  $\beta$  functions read [7]

$$\begin{aligned}\beta_u &\equiv \mu \frac{\partial u}{\partial \mu} = -\varepsilon u + (N+4)u^2 - 18uf + 54f^2, \\ \beta_f &\equiv \mu \frac{\partial f}{\partial \mu} = -\varepsilon f + Nf^2.\end{aligned}\quad (4)$$

One can easily verify that a stable fixed point exists only for  $N > N_c(\varepsilon)$ , with

$$N_c(\varepsilon) = N_4 + O(\varepsilon), \quad N_4 = 90 + 24\sqrt{15} \approx 183. \quad (5)$$

The corresponding zero of the  $\beta$  functions is

$$f^* = \frac{\varepsilon}{N}, \quad (6)$$

$$u^* = \frac{N + 18 + \sqrt{N^2 - 180N - 540}}{2N(N+4)} \varepsilon \approx \frac{\varepsilon}{N}. \quad (7)$$

The presence of a stable fixed point indicates that these systems may undergo a continuous transition if  $N$  is large enough [ $N > N_c(1)$  in three dimensions], in agreement with the direct large- $N$  analysis [8]. The qualitative picture obtained in the one-loop calculation is not changed by higher-order calculations. The perturbative expansion has been recently extended to four loops [26], obtaining  $N_c(\varepsilon)$  to  $O(\varepsilon^3)$ ,

$$N_c(\varepsilon) = N_4 [1 - 1.752\varepsilon + 0.789\varepsilon^2 + 0.362\varepsilon^3 + O(\varepsilon^4)]. \quad (8)$$

The large coefficients make a reliable three-dimensional ( $\varepsilon = 1$ ) estimate quite problematic. Nevertheless, by means of a resummation of the expansion, Ref. [26] obtained the estimate  $N_c = 12.2(3.9)$  in three dimensions, which confirms the absence of a stable fixed point for small values of  $N$ .

In the limit  $\beta_g \rightarrow \infty$ , the lattice AH model (3) is equivalent to the symmetric  $\text{O}(2N)$  vector theory. Therefore, for large  $\beta_g$  one expects significant crossover effects, which increase as  $\beta_g$  increases, due to the nearby  $\text{O}(2N)$  critical behavior. In the continuum AH model, the crossover is controlled by the RG flow in the vicinity of the  $\text{O}(2N)$  fixed point

$$u_{\text{O}(2N)}^* = \frac{1}{N+4}\varepsilon, \quad f = 0. \quad (9)$$

This fixed point exists for any  $N$  and is always unstable. The analysis of the stability matrix  $\Omega_{ij} = \partial\beta_i/\partial g_j$  shows

that it has a positive eigenvalue  $\lambda_u = \omega$ , where  $\omega > 0$  is the exponent controlling the leading scaling corrections in  $O(2N)$  vector models [20], and a negative eigenvalue, which gives the dimension of the operator that controls the crossover behavior,

$$\lambda_f = \left. \frac{\partial \beta_f}{\partial f} \right|_{f=0, u=u^*}. \quad (10)$$

Since the  $\beta$ -function  $\beta_f(u, f)$  associated with  $f$  has the general form

$$\beta_f = -\varepsilon f + f^2 F(u, f) \quad (11)$$

where  $F(u, f)$  has a regular perturbative expansion (see, e.g., the four-loop expansion reported in Ref. [26]), we obtain

$$\lambda_f = -\varepsilon \quad (12)$$

to all orders in perturbation theory. Therefore, the crossover exponent  $y_f = -\lambda_f$  is 1 in three dimensions. Note that these crossover features related to the unstable  $O(2N)$  fixed point are independent of the existence of the stable fixed point, which is only relevant to predict the eventual asymptotic behavior.

### B. Gauge-invariant Landau-Ginzburg-Wilson framework

An alternative field-theoretical approach is the LGW framework [15, 20, 28–31], in which one assumes that the relevant critical modes are associated with the gauge-invariant local composite site variable

$$Q_{\mathbf{x}}^{ab} = \bar{z}_{\mathbf{x}}^a z_{\mathbf{x}}^b - \frac{1}{N} \delta^{ab}, \quad (13)$$

which is a hermitian and traceless  $N \times N$  matrix. As discussed in Refs. [15, 19, 32], this is a highly non-trivial assumption, as it postulates that gauge fields do not play an important role in the effective theory. The order-parameter field in the corresponding LGW theory is therefore a traceless hermitian matrix field  $\Psi^{ab}(\mathbf{x})$ , which can be formally defined as the average of  $Q_{\mathbf{x}}^{ab}$  over a large but finite lattice domain. The LGW field theory is obtained by considering the most general fourth-order polynomial in  $\Psi$  consistent with the  $U(N)$  global symmetry:

$$\begin{aligned} \mathcal{H}_{\text{LGW}} = & \text{Tr}(\partial_\mu \Psi)^2 + r \text{Tr} \Psi^2 \\ & + w \text{tr} \Psi^3 + u (\text{Tr} \Psi^2)^2 + v \text{Tr} \Psi^4. \end{aligned} \quad (14)$$

Also in this framework continuous transitions may only arise if the RG flow in the LGW theory has a stable fixed point.

For  $N = 2$ , the cubic term in Eq. (14) vanishes and the two quartic terms are equivalent. Therefore, one recovers the  $O(3)$ -symmetric vector LGW theory, leading to

the prediction that the phase transition may be continuous and, in this case, that it belongs to the Heisenberg universality class. For  $N \geq 3$ , the cubic term is generally expected to be present. Its presence is usually taken as an indication that phase transitions occurring in this class of systems are generally of first order. Indeed, a straightforward mean-field analysis shows that the transition is of first order in four dimensions where mean field applies. If statistical fluctuations are small—this is the basic assumption—the transition should be of first order also in three dimensions. In this scenario, continuous transitions may still occur, but they require a fine tuning of the microscopic parameters leading to the effective cancellation of the cubic term. These arguments were originally [15, 18] applied to predict the behavior of  $CP^{N-1}$  models. However, as they are only based on symmetry considerations, they can be extended to AH lattice models, as well.

### C. Comparison of the alternative field-theoretical approaches

The two field-theoretical approaches outlined above give inconsistent predictions both for small and large values of  $N$ . The contradiction is quite striking for the two-component  $N = 2$  case. For this value of  $N$ , the continuum AH model predicts the absence of continuous transitions, due to the absence of a stable fixed point. On the other hand, a stable fixed point—it is the usual Heisenberg  $O(3)$  fixed point—exists in the effective LGW theory based on a gauge-invariant order parameter, leaving open the possibility of observing continuous transitions (first-order transitions are never excluded as the statistical model may be outside the attraction domain of the fixed point). The numerical results for the  $CP^1$  lattice models [15, 16], as well as the AH lattice results we shall present below, confirm the existence of continuous transitions in models with  $N = 2$ : the LGW theory provides the correct description of the large-scale behavior of these systems. There are at least two possible explanations for the failure of the continuum AH model. A first possibility is that it does not encode the relevant degrees of freedom at the transition. A second possibility is that the problem is not in the continuum AH model, but rather in the perturbative treatment around four dimensions. The three-dimensional fixed point may not be analytically related to a four-dimensional fixed point, and therefore it escapes any perturbative analysis in powers of  $\varepsilon$ .

We also recall that the perturbative AH approach of Sec. II A also fails for  $N = 1$ . Although no stable fixed point is identified in the  $\varepsilon$  expansion, see Sec. II A, these models may undergo continuous transitions in the XY universality class [9–11]. It is worth mentioning that there are also other systems in which the  $\varepsilon$  expansion fails to provide the correct physical picture in three dimensions. We mention the  $\phi^4$  theories describing frustrated spin models with noncollinear order [33, 34] and

the  $^3\text{He}$  superfluid transition from the normal to the planar phase [35].

For large values of  $N$ , the continuum AH theory and the effective LGW approach give again contradictory results. Indeed, the former approach indicates that continuous transitions are possible, a prediction which is supported by the large- $N$  analysis of lattice models, see, e.g., Ref. [15]. If one trusts the argument based on the relevance of the cubic term, the LGW approach predicts instead a first-order transition, unless a fine tuning of the microscopic parameters is performed. Again, there are two possible explanations for the different conclusions obtained in the LGW approach. A first possibility is that the critical modes at the transition are not exclusively associated with the gauge-invariant order parameter  $Q$  defined in Eq. (13). Other features, for instance the gauge degrees of freedom, may become relevant, requiring an effective description different from that of the LGW theory (14). If this interpretation is correct, the continuum AH model would be the correct theory as it includes the gauge fields explicitly. A second possibility is that the presence of a cubic term in the LGW Hamiltonian does not necessarily imply the absence of continuous transitions in three dimensions, as it is usually assumed. It might be that statistical fluctuations soften the transition as one moves from four to three dimensions; see, e.g., Refs. [16, 17] for a discussion of this issue.

While the two field-theoretical approaches give different predictions for  $N = 1, 2$  and  $N$  large (more precisely, for  $N > N_c$ , see Sec. II A), for  $3 \leq N < N_c$  they both predict that all models undergo a first-order transition. For  $N = 3$  simulation results do not presently confirm it. Indeed, while numerical results for the lattice model with Hamiltonian (3) and  $\beta_g = 0$  show a robust indication that the transition is of first order [15], the results for the loop model considered in Refs. [16, 17] apparently favor a continuous transition. The available numerical results for lattice  $\text{CP}^3$  models, i.e., for  $N = 4$ , are generally consistent with first-order transitions [6, 15, 17]. We also mention that Ref. [6] claims that the AH lattice model (3) undergoes a continuous transition for  $\beta_g = 1$  and  $N = 4$ , a result which is at odds with the above arguments. However, as we shall show, the numerical results that we present later do not confirm their conclusions, but are instead consistent with a relatively weak first-order transition.

### III. NUMERICAL RESULTS

#### A. Numerical simulations and observables

In this section we present a finite-size scaling (FSS) analysis of numerical results of Monte Carlo (MC) simulations for  $N = 2$  and  $N = 4$ . For this purpose we consider cubic lattices of linear size  $L$  with periodic boundary conditions. We study the behavior of the system as a function of  $\beta$  at fixed  $\beta_g$ .

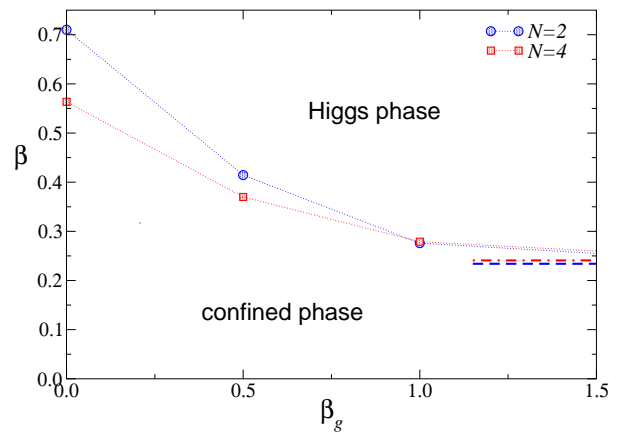


FIG. 1: The phase diagram of the AH lattice model in the space of parameters  $\beta$  and  $\beta_g$ , for  $N = 2$  and  $N = 4$ . The points are the MC estimates of the critical points, the dotted lines that connect them are only meant to guide the eye. The horizontal lines indicate the limiting values of  $\beta_c$  for  $\beta_g \rightarrow \infty$  for  $N = 2$  ( $\beta_c \approx 0.23396$ , dashed) and  $N = 4$  ( $\beta_c \approx 0.24084$ , dot-dashed): they correspond to the critical  $\beta_c$  for the standard three-dimensional  $O(4)$  and  $O(8)$  vector models, respectively. For  $\beta_g = 0$ , we have [15]  $\beta_c = 0.7102(1)$  ( $N = 2$ ) and  $\beta_c = 0.5636(1)$  ( $N = 4$ ).

The linearity of Hamiltonian (3) with respect to each lattice variable allows us to employ an overrelaxed algorithm for the updating of the lattice configurations. It consists in a stochastic mixing of microcanonical and standard Metropolis updates of the lattice variables [36–38]. To update each lattice variable, we randomly choose either a standard Metropolis update, which ensures ergodicity, or a microcanonical move, which is more efficient than the Metropolis one but does not change the energy. On average, we perform three/four microcanonical updates for every Metropolis proposal. In the Metropolis update, changes are tuned so that the acceptance is  $1/3$ .

We compute the energy density and the specific heat, defined as

$$E = \frac{1}{NV} \langle H \rangle, \quad C = \frac{1}{N^2 V} (\langle H^2 \rangle - \langle H \rangle^2), \quad (15)$$

where  $V = L^3$ . We consider correlations of the hermitean gauge invariant operator (13). Its two-point correlation function is defined as

$$G(\mathbf{x} - \mathbf{y}) = \langle \text{Tr} Q_{\mathbf{x}} Q_{\mathbf{y}} \rangle, \quad (16)$$

where the translation invariance of the system has been taken into account. The susceptibility and the correlation length are defined as  $\chi = \sum_{\mathbf{x}} G(\mathbf{x})$  and

$$\xi^2 \equiv \frac{1}{4 \sin^2(\pi/L)} \frac{\tilde{G}(\mathbf{0}) - \tilde{G}(\mathbf{p}_m)}{\tilde{G}(\mathbf{p}_m)}, \quad (17)$$

where  $\tilde{G}(\mathbf{p}) = \sum_{\mathbf{x}} e^{i\mathbf{p} \cdot \mathbf{x}} G(\mathbf{x})$  is the Fourier transform of  $G(\mathbf{x})$ , and  $\mathbf{p}_m = (2\pi/L, 0, 0)$  is the minimum nonzero lat-

tice momentum. We also consider the Binder parameter

$$U = \frac{\langle \mu_2^2 \rangle}{\langle \mu_2 \rangle^2}, \quad \mu_2 = \sum_{\mathbf{x}, \mathbf{y}} \text{Tr} Q_{\mathbf{x}} Q_{\mathbf{y}}. \quad (18)$$

We consider correlations of the fundamental variable  $\mathbf{z}_x$ . To obtain a gauge-invariant quantity, we consider correlations with  $\lambda$  strings, i.e., averages like

$$\text{Re} \left\langle \bar{\mathbf{z}}_{\mathbf{x}} \cdot \mathbf{z}_{\mathbf{y}} \prod_{\ell \in \mathcal{C}} \lambda_{\ell} \right\rangle, \quad (19)$$

where the product extends over the link variables that belong to a lattice path  $\mathcal{C}$  connecting points  $\mathbf{x}$  and  $\mathbf{y}$ . To define quantities that have the correct FSS, the path  $\mathcal{C}$  must be chosen appropriately, as discussed in Ref. [39]. Here, to simplify the calculations, we only consider correlations between points that belong to lattice straight lines. We define

$$G_V(d, L) = \frac{1}{V} \sum_{\mathbf{x}} \text{Re} \left\langle \bar{\mathbf{z}}_{\mathbf{x}} \cdot \mathbf{z}_{\mathbf{x}+d\hat{\mu}} \prod_{n=0}^{d-1} \lambda_{\mathbf{x}+n\hat{\mu}, \mu} \right\rangle, \quad (20)$$

where all coordinates should be taken modulo  $L$  because of the periodic boundary conditions. Note that in the definition of  $G_V$  we average over all lattice sites  $\mathbf{x}$  exploiting the translation invariance of systems with periodic boundary conditions, and select a generic lattice direction  $\hat{\mu}$  (in our MC simulations we also average over the three equivalent directions). Note also that  $G_V(0, L) = 1$  and that  $G_V(L, L)$  is the average value  $P(L)$  of the Polyakov loop,

$$P(L) = \frac{1}{V} \sum_{\mathbf{x}} \text{Re} \left\langle \prod_{n=0}^{L-1} \lambda_{\mathbf{x}+n\hat{\mu}, \mu} \right\rangle. \quad (21)$$

Finally, we consider the so-called Wilson loop defined as

$$W(m, L) = \text{Re} \left\langle \prod_{\ell \in \mathcal{C}} \lambda_{\ell} \right\rangle, \quad (22)$$

where the path  $\mathcal{C}$  is a square of linear size  $m$ .

In the following we present a FSS analysis of the above observables, for  $N = 2$  and  $N = 4$  and some values of  $\beta_g > 0$ . In Fig. 1 we anticipate the resulting phase diagrams. For both  $N = 2$  and  $4$ ,  $\beta_c$  decreases as  $\beta_g$  increases and, eventually, it converges to the value appropriate for the  $n$ -vector model with  $n = 4$  and  $8$ ,  $\beta_c = 0.233965(2)$  [40, 41] and  $\beta_c = 0.24084(1)$  [18].

As we shall discuss, our numerical data are consistent with a simple scenario in which the nature of the transitions along the line separating the confined and Higgs phases is unchanged for any finite  $\beta_g \geq 0$ . Therefore, for  $N = 2$  the phase transitions are continuous and belong to the Heisenberg universality class as it occurs in the  $\text{CP}^1$  model. The  $\text{O}(4)$  critical behavior occurs only for  $\beta_g$  strictly equal to  $\infty$ . For  $N = 4$  instead, transitions are of first order, except for  $\beta_g = \infty$ , where the system develops an  $\text{O}(8)$  vector critical behavior.

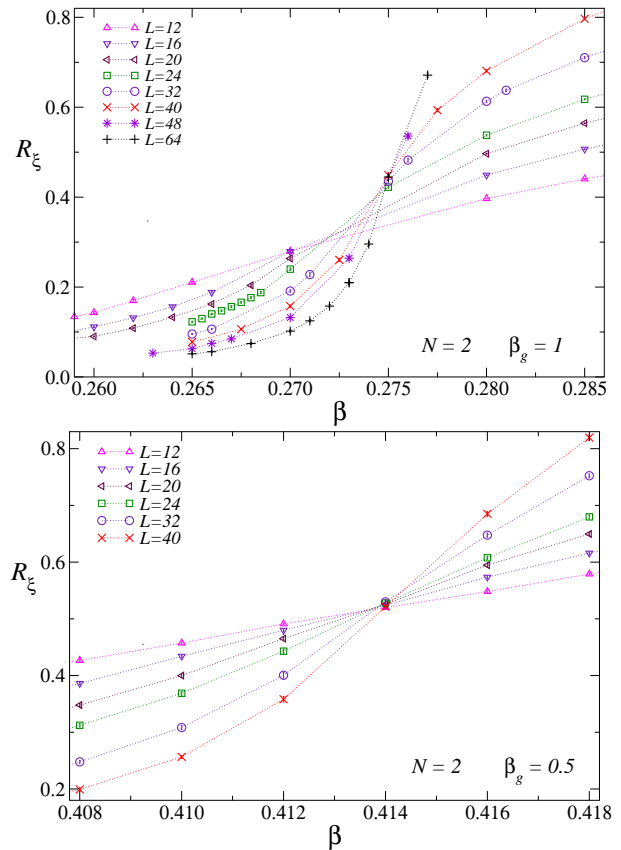


FIG. 2:  $R_{\xi}$  versus  $\beta$  for the  $N = 2$  AH lattice model, for  $\beta_g = 0.5$  (bottom) and  $\beta_g = 1$  (top). In both cases the data for different values of  $L$  show a crossing point, whose position provides an estimate of the critical point:  $\beta_c = 0.4145(5)$  and  $\beta_c = 0.276(1)$  for  $\beta_g = 0.5$  and  $\beta_g = 1$ , respectively.

## B. Continuous transitions for $N = 2$

As already mentioned, lattice versions of the three-dimensional  $\text{CP}^1$  model undergo continuous transitions belonging to the Heisenberg universality class, i.e., that of the standard  $N = 3$  vector model. This has been also shown [15] for model (3) with  $\beta_g = 0$  [ $\beta_c = 0.7102(1)$  in this case]. On the other hand, for  $\beta_g = \infty$  the model is equivalent to the standard  $\text{O}(4)$  vector model that has a continuous transition for [40, 41]  $\beta_c = 0.233965(2)$ . As already inferred from the RG flow of the AH continuum theory, the  $\beta_g = \infty$   $\text{O}(4)$  critical behavior is expected to be unstable against perturbations associated with nonzero values of  $\beta_g^{-1}$ . Therefore, the most natural hypothesis is that the all transitions for finite  $\beta_g \geq 0$  belong to the Heisenberg universality class. However, a substantial crossover from the  $\text{O}(4)$  to the  $\text{O}(3)$  behavior is expected to characterize the transition for relatively large values of  $\beta_g$ ,  $\beta_g \gtrsim 1$  say.

To provide evidence of this scenario, we perform MC simulations for  $\beta_g = 0.5$  and  $1$ . As in our previous work [15], we study the FSS behavior of the Binder parameter  $U$  and of  $R_{\xi} = \xi/L$ . At continuous transitions the FSS

limit is obtained by taking  $\beta \rightarrow \beta_c$  and  $L \rightarrow \infty$  keeping

$$X \equiv (\beta - \beta_c)L^{1/\nu} \quad (23)$$

fixed. Any RG invariant quantity  $R$ , such as  $R_\xi \equiv \xi/L$  and  $U$ , is expected to asymptotically behave as

$$R(\beta, L) = f_R(X) + O(L^{-\omega}), \quad (24)$$

where  $\omega > 0$  is the leading scaling correction exponent [20], and  $f_R(X)$  is universal apart from a normalization of its argument. The function  $f_R(X)$  only depends on the shape of the lattice and on the boundary conditions. In the case of the Heisenberg universality we have [20, 42–44]  $\nu = 0.7117(5)$  and  $\omega = 0.78(1)$ . As  $R_\xi$  is monotonically increasing as a function of  $X$ , Eq. (24) implies that

$$U = F(R_\xi) + O(L^{-\omega}), \quad (25)$$

where  $F(x)$  is a universal scaling function. As in our previous work [15], we will use Eq. (25) to perform a direct check of universality, because no model-dependent normalizations enter: If two models belong to the same universality class, the data for both of them should collapse onto the same curve as  $L$  increases. The only difficulty in the approach is that one should be careful in identifying corresponding operators in the two models.

To identify the correct operators, one may reason as follows. In the AH lattice model the basic quantity that we consider is the local operator (13). To identify the corresponding operator in the Heisenberg model, we use the explicit relation between the  $CP^1$  and the  $O(3)$  vector model. Under the mapping, the parameter  $U$  and  $\xi$  correspond to the usual  $O(3)$  vector Binder parameter and correlation length (i.e., computed from correlations of the fundamental spin variable  $\mathbf{s}_x$ ). The mapping of the large- $\beta_g$  limit of the AH lattice model into the  $O(4)$  vector model is instead more complex and is discussed in detail in App. A and in the supplementary material [25]. The correspondence is not trivial and  $U$  is identified with a combination of suitably defined  $O(4)$  tensor Binder parameters.

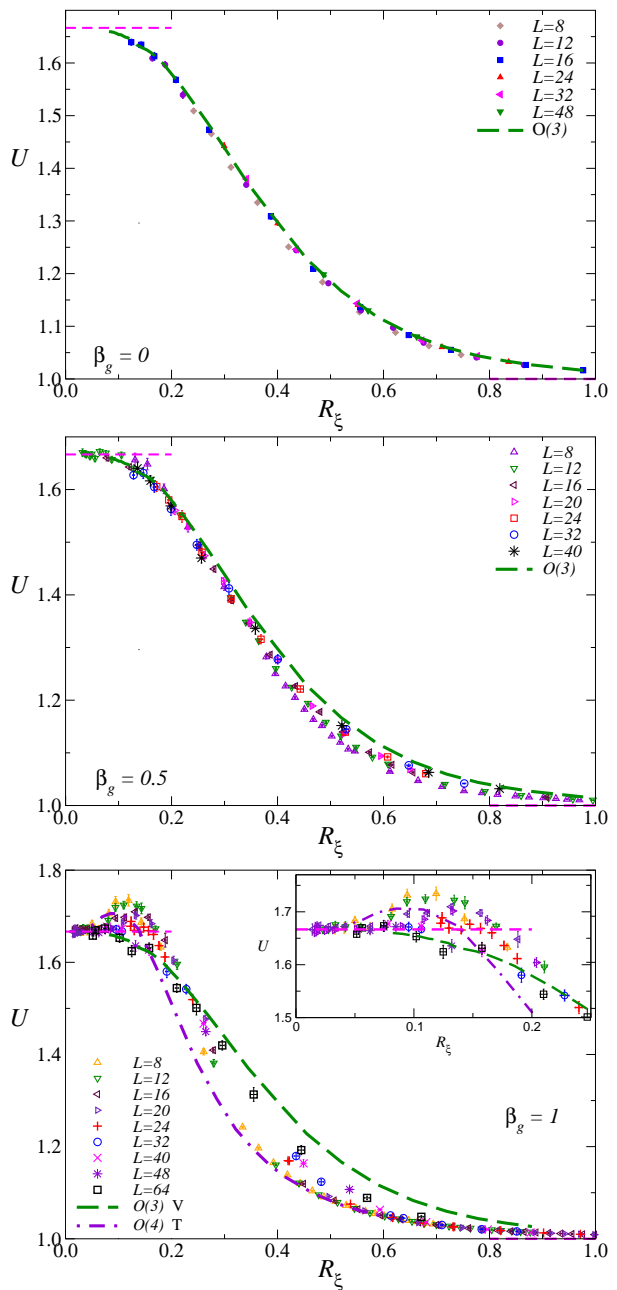


FIG. 3: The Binder parameter  $U$  versus  $R_\xi$  for the  $N = 2$  AH lattice model, and for  $\beta_g = 0$  (top, data from Ref. [15]),  $\beta_g = 0.5$  (middle) and  $\beta_g = 1$  (bottom). In all panels the dashed line is the Heisenberg curve, as obtained from MC simulations of the  $O(3)$  vector model. The dot-dashed line in the lower panel is the limiting curve for  $\beta_g \rightarrow \infty$  (see App. A). The inset enlarges the region  $R_\xi < 0.25$ , showing that the nonmonotonic behavior that characterizes the small-size data (similar to the one of the  $O(4)$  curve) for  $R_\xi \approx 0.1$  disappears with increasing  $L$ . The horizontal dashed line shows the asymptotic value  $U(R_\xi \rightarrow 0) = 5/3$ .

In Fig. 2 we plot  $R_\xi$  versus  $\beta$ , for several values of  $L$ . The data for different values of the size  $L$  show crossing points, which provide estimates of the critical point:  $\beta_c = 0.4145(5)$  and  $\beta_c = 0.276(1)$  for  $\beta_g = 0.5$  and

$\beta_g = 1$ , respectively. Data are consistent with a continuous transition.

We now argue that the transitions are consistent with the expected asymptotic Heisenberg behavior. The best evidence is provided by the plots of  $U$  versus  $R_\xi$ , see Fig. 3. In all panels we report the data and the corresponding O(3) curve. If our simple scenario is correct, the data for all values of  $\beta_g$  must approach the O(3) curve with increasing  $L$ . For  $\beta_g = 0$  we observe very good agreement, as already discussed in Ref. [15]. For  $\beta_g = 0.5$  convergence is slower, indicating that scaling corrections increase with increasing  $\beta_g$ . For  $R_\xi \lesssim 0.25$  we observe a good collapse of the data, while in the opposite case, we observe a clear upward trend, consistent with an asymptotic O(3) behavior. For  $\beta_g = 1$ , for small values of  $L$  we observe significant differences between data and O(3) curve. These discrepancies can be explained by scaling corrections. For  $R_\xi \lesssim 0.25$ , the results for  $L = 64$  fall on top of the O(3) scaling curve, as predicted. For larger values of  $R_\xi$ , crossover effects are stronger, but the trend of the data is the expected one.

To be more quantitative, let us note that, for large values of  $L$ , the Binder parameter  $U$  should behave as [20]

$$U(\beta, \beta_g, L) = F(R_\xi) + a(\beta_g) G(R_\xi) L^{-\omega} + \dots \quad (26)$$

where  $F(R_\xi)$  is the O(3) scaling function,  $G(R_\xi)$  is a universal function, and  $a(\beta_g)$  is a constant that encodes the  $\beta_g$ -dependent size of the leading scaling corrections decaying as  $L^{-\omega}$ . We have verified that our data for  $\beta_g = 0.5$  and 1 are consistent with Eq. (26), if we take  $\omega = 0.78$  (the leading correction-to-scaling exponent in Heisenberg systems [20, 42–44]) and  $a(1)/a(0.5) \approx 5$ . This can be checked from Fig. 4, where we report

$$\Delta(\beta, \beta_g, L) = \frac{1}{a(\beta_g)} L^\omega [U(\beta, \beta_g, L) - F(R_\xi)], \quad (27)$$

where  $F(R_\xi)$  has been determined in the O(3) vector model,  $\omega = 0.78$ ,  $a(1) = 5$ , and  $a(0.5) = 1$ . All data reported in the figure are consistent with a single scaling curve that would be identified with the function  $G(R_\xi)$  in Eq. (26). The existence of similar crossover effects for  $\beta_g = 0.5$  and 1 is another demonstration of universality.

It is interesting to note that the behavior of the data for small  $L$  at  $\beta_g = 1$  can be interpreted as due to the presence of O(4) fixed point that controls the critical behavior for  $\beta_g \rightarrow \infty$ . In the lower panel of Fig. 3, we also plot the O(4) scaling curve. The data for  $\beta_g = 1$  apparently follow the O(4) curve for small lattice sizes, and then move toward the O(3) curve with increasing  $L$ . In particular, note the nonmonotonic behavior of the data for small lattice sizes and  $R_\xi \approx 0.1$ , similar to the one that characterizes the O(4) curve. Such a behavior disappears with increasing  $L$  (see the inset in the lower panel of Fig. 3).

On the basis of the above numerical results we argue that the finite-temperature transition is continuous for any finite  $\beta_g \geq 0$  and belongs to the Heisenberg universality class. However, for relatively large values of  $\beta_g$ , say

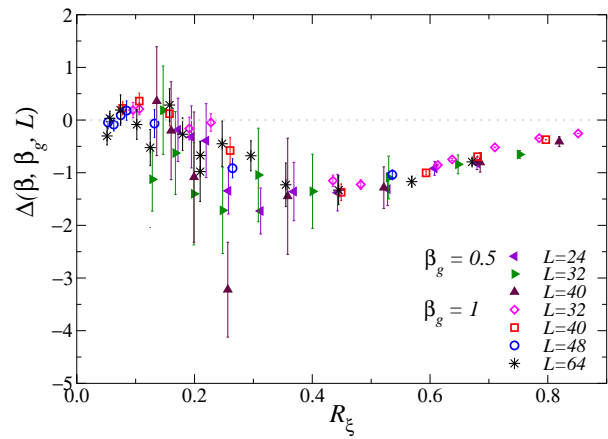


FIG. 4: The quantity  $\Delta(\beta, \beta_g, L)$  defined in Eq. (27) versus  $R_\xi$ . We report data for  $\beta_g = 1$  and 0.5 and several values of  $L$ .

$\beta_g \gtrsim 1$ , notable crossover effects emerge. They are apparently related to the presence of the O(4) fixed point, which is the relevant one  $\beta_g \rightarrow \infty$ . For large values of  $\beta_g$ , such effects may hide the asymptotic Heisenberg behavior. For intermediate sizes, data are expected to show an effective O(4) critical behavior, converging to the Heisenberg behavior only for very large lattices.

### C. First-order transitions for $N = 4$

We now discuss the behavior of the  $N = 4$  AH lattice model, providing evidence that the transitions along the line separating the Higgs and confined phases are of first order for any finite  $\beta_g$ . Only when  $\beta_g$  is strictly infinity is the transition continuous: it belongs to the O(8) vector universality class.

As shown in Ref. [15], the transition is of first order for  $\beta_g = 0$ . To show that the nature of the transition is unchanged for  $\beta_g > 0$ , we first consider the specific heat and the Binder parameter  $U$ . Both of them are expected to increase as the volume at a first-order transition. Indeed, according to the standard phenomenological theory [45], for a lattice of size  $L$  there exists a value  $\beta_{\max, C}(L)$  of  $\beta$  where  $C$  takes its maximum value  $C_{\max}(L)$ , which asymptotically increases as

$$C_{\max}(L) = V \left[ \frac{1}{4} \Delta_h^2 + O(1/V) \right], \quad (28)$$

$$\beta_{\max, C}(L) - \beta_c \approx c V^{-1}, \quad (29)$$

where  $V = L^d$  and  $\Delta_h$  is the latent heat [defined as  $\Delta_h = E(\beta \rightarrow \beta_c^+) - E(\beta \rightarrow \beta_c^-)$ ]. Analogously, the behavior of the Binder parameter  $U(\beta, L)$  is expected to show a maximum  $U_{\max}(L)$  at fixed  $L$  (for sufficiently large  $L$ ) at  $\beta = \beta_{\max, U}(L) < \beta_c$  with [15, 33, 46]

$$U_{\max} \sim a V + O(1), \quad (30)$$

$$\beta_{\max, U}(L) - \beta_c \approx b V^{-1}. \quad (31)$$

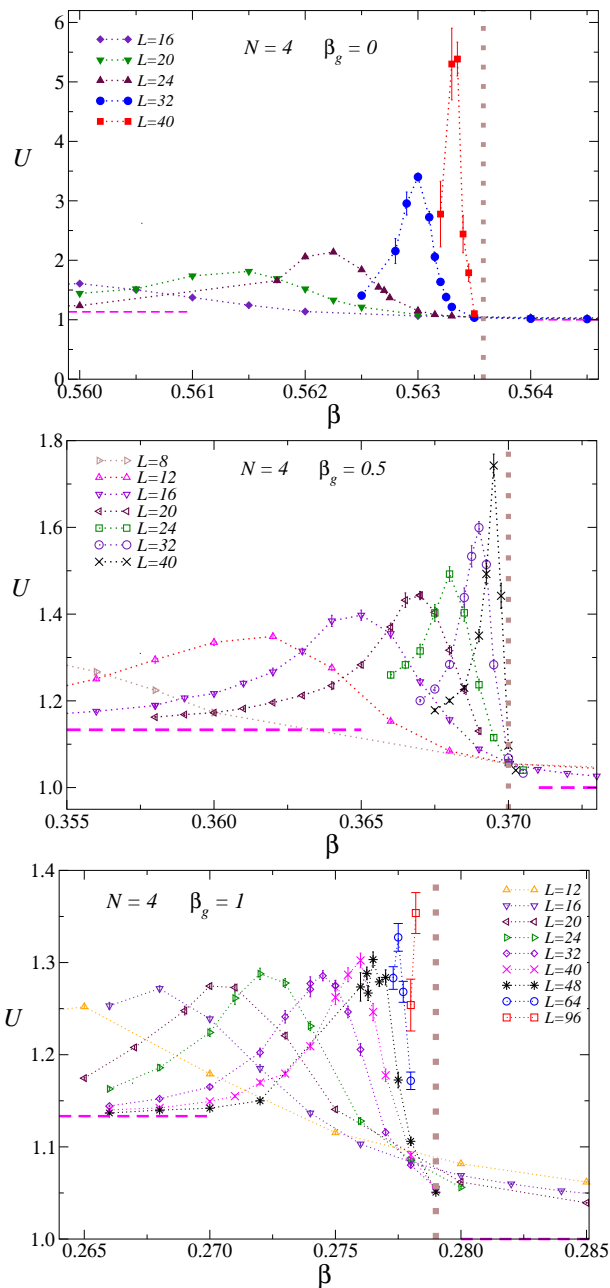


FIG. 5: Plot of the Binder parameter  $U$  versus  $\beta$ , for  $\beta_g = 0$  (top, from Ref. [15]),  $\beta_g = 1/2$  (middle), and  $\beta_g = 1$  (bottom), for  $N = 4$ . The vertical lines correspond to the estimates of the transition points. The horizontal dashed lines show the values  $U(\beta \rightarrow 0) = 17/15$  and  $U(\beta \rightarrow \infty) = 1$ .

The previous relations are valid in the asymptotic limit and, for weak transitions, require data on large lattices. As we discussed in Ref. [15], one can identify first-order transitions on significantly smaller lattices from the analysis of the behavior of the Binder parameter  $U$ . In the presence of a first-order transition, one observes large violations of the scaling relation (25) for values of  $L$  that are significantly smaller than those at which relations (28) and (31) hold. We will follow this approach here,

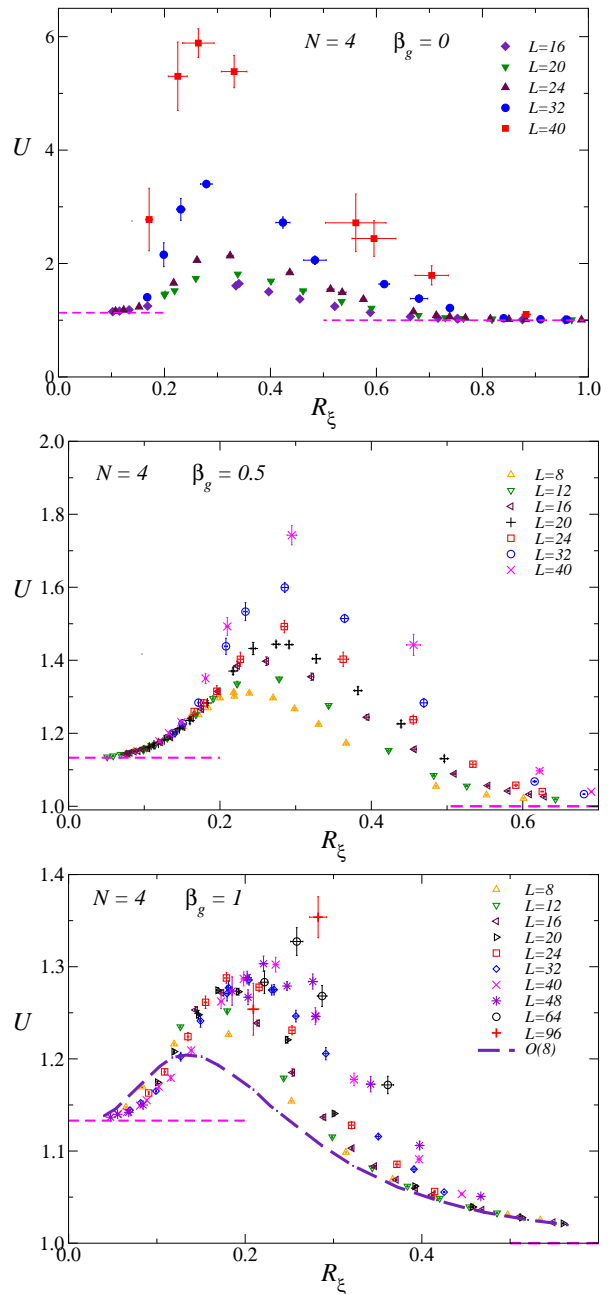


FIG. 6: The Binder parameter  $U$  versus  $R_\xi$  versus  $\beta$ , for  $\beta_g = 0$  (top, from Ref. [15]),  $\beta_g = 1/2$  (middle), and  $\beta_g = 1$  (bottom) for  $N = 4$ . The dashed line in the lower panel is the  $O(8)$  limiting scaling curve, see App. A. The horizontal dashed lines show the asymptotic values  $U(R_\xi \rightarrow 0) = 17/15$  and  $U(R_\xi \rightarrow \infty) = 1$ .

considering again two values of  $\beta_g$ , 0.5 and 1.

In Fig. 5 we report numerical estimates of  $U$  at  $\beta_g = 0$  (taken from Ref. [15]),  $\beta_g = 0.5$ , and  $\beta_g = 1$ . Clearly, the maximum  $U_{\max}$  increases with increasing  $L$ , as expected for a first-order transition. However, with increasing  $\beta_g$ , the rate of increase becomes smaller, indicating that the transition becomes weaker. The specific heat behaves

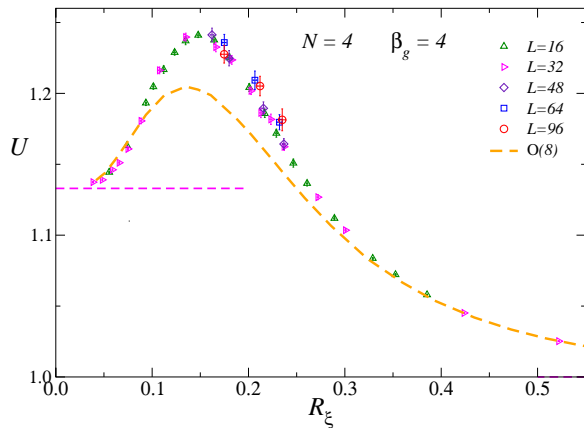


FIG. 7: The Binder parameter  $U$  versus  $R_\xi$  for  $\beta_g = 4$  and  $N = 4$ . The full line connects the data with  $L = 16$ . The dashed line is the O(8) limiting scaling curve, see App. A.

analogously.

To obtain a better evidence that the finite-size behavior is not compatible with a continuous transition, we plot  $U$  versus  $R_\xi$ , see Fig. 6. Data do not show any scaling behavior, as expected at a first-order transition.

Note that for  $\beta_g = 1$  the small size data show an apparent scaling behavior for small values of  $R_\xi$  and small  $L$ , which may lead to erroneous conclusions when limiting the FSS analysis to small lattices (as in Ref. [6]). To clarify the origin of the transient effects, and understand whether they can be interpreted as due to the O(8) fixed point that controls the behavior for  $\beta_g = \infty$ , we have performed MC simulations for  $\beta_g = 4$ . This value is so large that, for our range of values of  $L$ , we do not expect to observe effects related to the first-order nature of the transition and therefore all data should be in the crossover region. The analysis of  $U$  as a function of  $\beta$  allows us to estimate  $\beta_c = 0.2484(2)$ , which is close to the O(8) value,  $\beta_c \approx 0.2408$ . At the transition, gauge fields are significantly ordered and indeed, the average value of the product of the gauge fields along an elementary plaquette (a Wilson loop of size 1) is 0.95780(5) (for comparison, such a product is equal to 0.8235(5) at the transition for  $\beta_g = 1$ ). In Fig. 7 we report  $U$  versus  $R_\xi$  and compare it with the O(8) curve. The numerical data with  $16 \leq L \leq 48$  apparently fall onto a single scaling curve, while the data corresponding to  $L = 64$  and  $96$  begin to show the drift that characterizes the results at  $\beta_g \leq 1$  and which is related to the asymptotic first-order nature of the transition. The apparent scaling curve for small values of  $L$  is different from the O(8) one, indicating that for  $\beta_g = 4$  we are observing a sizable contribution due the relevant operator that destabilizes the O(8) fixed point for finite  $\beta_g$ . We can also infer from the substantial stability of the results for  $L \leq 48$  that it has a very small (positive) scaling dimensions  $y$ . Indeed, close to the O(8) fixed point, we expect

$$U(\beta, \beta_g) = F(R_\xi, b(\beta_g, \beta)L^y), \quad (32)$$

where  $b(\beta_g, \beta)$  is a nonuniversal amplitude, which vanishes for  $\beta_g \rightarrow \infty$ . For each  $\beta_g$  the crossover region is the one in which  $b(\beta_g, \beta)L^y \ll 1$ . If this condition holds,  $U$  can be written as

$$U(\beta, \beta_g) = F(R_\xi, 0) + b(\beta_g, \beta)L^y G(R_\xi), \quad (33)$$

where the first term is the O(8) scaling function. This equation would imply that the deviations from the O(8) behavior scale, at least for  $\beta_g$  very large, as  $L^y$ . Our results therefore imply that  $y$  should be small enough, so that  $L^y$  does not change significantly as  $L$  varies from 16 to 48.

In conclusion, the numerical results favor a phase diagram based on a first-order transition line for  $\beta_g > 0$ , starting from the first-order transition of the CP<sup>3</sup> models, corresponding to  $\beta_g = 0$ . With increasing  $\beta_g$  the first-order transition becomes weaker. We observe substantial crossover phenomena for  $\beta_g \gtrsim 1$ . They may be explained in terms of the O(8) fixed point controlling the behavior for  $\beta_g \rightarrow \infty$ , perturbed by a relevant operator with a relatively small scaling dimension.

#### D. Vector and gauge observables

In the previous sections we discussed the behavior of quantities defined in terms of the gauge-invariant order parameter  $Q_x^{ab}$ . Here we discuss instead the vector correlation function (20) and the gauge observables (21) and (22). We focus on  $N = 4$ .

Let us first discuss their behavior in the two different phases. In the high-temperature phase  $\beta < \beta_c$ , we find that the correlation function can be approximated as ( $x > 0$ )

$$G_V(x, L) = A e^{-x/\xi_z}, \quad (34)$$

as soon as  $x$  is 2 or 3. Moreover, for small  $\beta$ ,  $\xi_z$  is very little dependent on  $\beta_g$ . For instance, for  $\beta = 0.1$ , the strong-coupling behavior  $G_V(x, L) \sim (N\beta)^x$  holds quite precisely for all values of  $\beta_g$ . Wilson loops behave in a very similar fashion. We find  $W(m, L) \approx B \exp(-4m/\xi_w)$  with  $\xi_w \approx \xi_z$  as long as  $m \gtrsim 2$ . Clearly, in the high-temperature phase a single gauge mode controls the behavior of all observables that involve gauge degrees of freedom.

The behavior in the low-temperature phase is analogous. The correlation function  $G_V(x, L)$  behaves as in Eq. (34); see the upper panel of Fig. 8 for results at  $\beta = 0.8$ . Moreover, Polyakov and Wilson loops satisfy

$$P(L) = A e^{-L/\xi_z}, \quad W(m) = B e^{-4m/\xi_z}, \quad (35)$$

with the same correlation length and  $A, B \approx 1$ . Fig. 8 also shows that  $G_V(x, L)$  has a very precise exponential decay even when  $\xi_z \gtrsim L$ . Clearly, it couples to a single isolated mode and hence there are no corrections to the leading exponential behavior. In this phase the correlation length increases with  $\beta_g$  (see the lower panel of

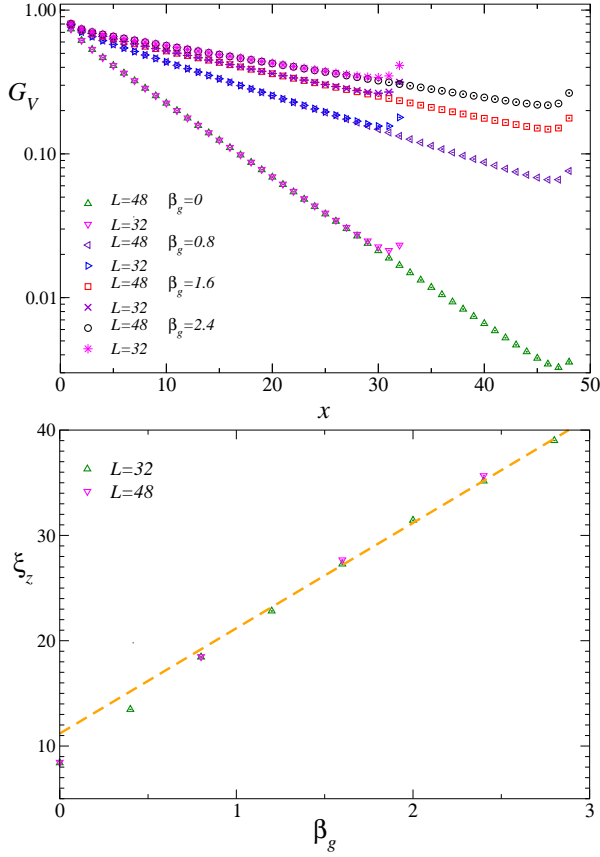


FIG. 8: Top: Vector correlation function  $G_V(x, L)$  versus  $x$  for  $\beta = 0.8$  and several values for  $\beta_g$ . Bottom: Vector correlation length  $\xi_z$  as a function of  $\beta_g$  for  $\beta = 0.8$ . The line shows that  $\xi_z$  scales as  $\beta_g$  for large  $\beta_g$  (the parameters have been determined by performing a linear fit of the data with  $\beta_g \geq 1.6$ ). For  $x = L$ ,  $G_V(L, L)$  corresponds to the average of the Polyakov loop.

Fig. 8): in agreement with perturbation theory, it scales linearly with  $\beta_g$  in the limit  $\beta_g \rightarrow \infty$ . Note the  $\xi_z$  is also expected to diverge in the limit  $\beta \rightarrow \infty$  at fixed  $\beta_g$ . Indeed, for  $\beta \rightarrow \infty$ , the relevant configurations are those that minimize the Hamiltonian term that depends on the fields  $\mathbf{z}$ . If we perform a local minimization on each link, we find the constraint

$$z_{\mathbf{x}+\hat{\mu}} = \bar{\lambda}_{\mathbf{x},\mu} z_{\mathbf{x}}. \quad (36)$$

This constraint can be satisfied simultaneously on the four links belonging to a plaquette only if the product of the gauge fields along the plaquette is 1. Analogously, the constraint is satisfied on the links that belong to a loop that wraps around the lattice only if the Polyakov operator is 1. It follows that gauge configurations are trivial— $\lambda_{\mathbf{x},\mu}$  is 1 on all links modulo gauge transformations—and  $\xi_z$  is infinite in this limit.

These results for the gauge observables indicate that gauge and vector observables are noncritical in both phases and that their behavior is analogous for small and large values of  $\beta$ . Only the limit  $\beta_g \rightarrow \infty$  distin-

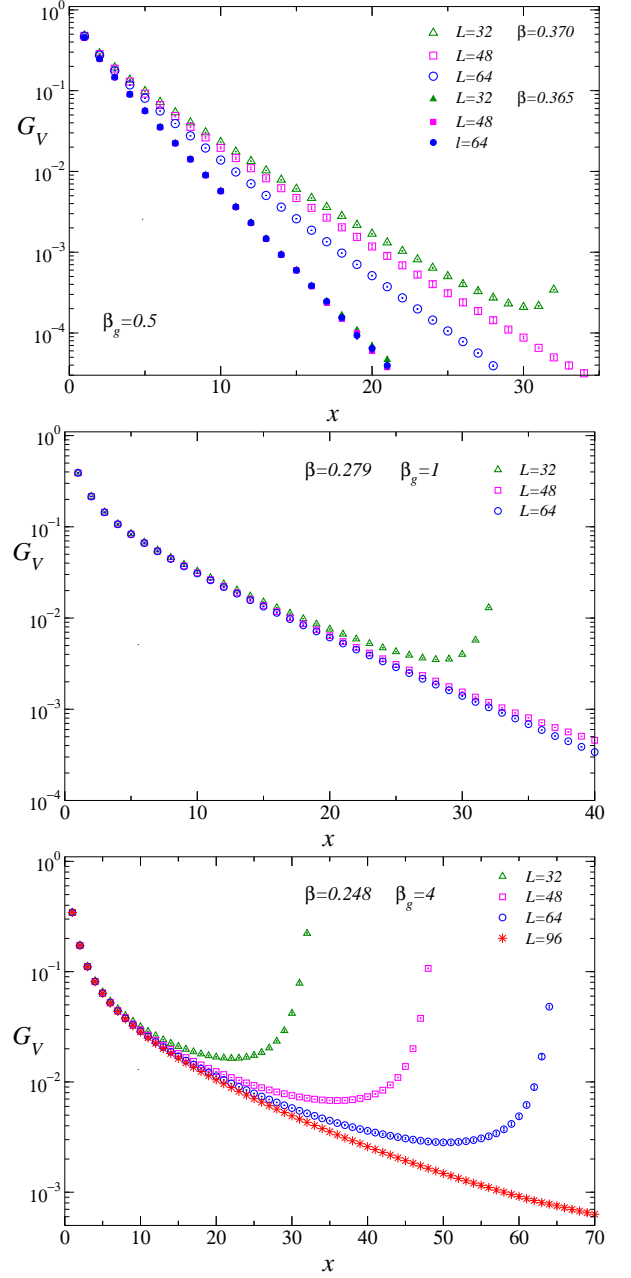


FIG. 9: The vector correlation function  $G_V(x, L)$  in the critical region for  $\beta_g = 0.5$  (top), 1 (middle) and 4 (bottom). For  $\beta_g = 0.5$  we report the estimate for  $\beta = 0.365$  (high-temperature phase) and for  $\beta = 0.370$  (low-temperature phase). For  $\beta_g = 1$  and 4, we report an effective estimate of the correlation function in the coexistence region (see text for a discussion), computed at  $\beta = 0.279$  for  $\beta_g = 1$ , and at  $\beta = 0.248$  for  $\beta_g = 4$ .

guishes the two sectors. If  $\beta_{c,\infty}$  is the transition point for  $\beta_g \rightarrow \infty$  [therefore in the  $O(2N)$  theory], for  $\beta_g \rightarrow \infty$ , the correlation length  $\xi_z$  is finite for  $\beta < \beta_{c,\infty}$  and infinite in the opposite case. This guarantees that vector correlations are critical in the  $O(2N)$  theory with a finite low-temperature magnetization. But this only occurs for

$\beta_g$  strictly equal to infinity. For finite  $\beta_g$ , only  $Q$  correlations display criticality.

Finally, let us discuss the behavior of vector and gauge quantities along the transition line. For  $N = 4$ , as we are dealing with first-order transitions, we expect  $G_V(x, L)$  to depend on the phase one considers. In the  $\text{CP}^3$  model ( $\beta_g = 0$ ) the transition is strong and therefore the high-temperature (HT) and low-temperature (LT) correlation functions can be easily computed by fixing  $\beta$  in the coexistence region and starting the simulation from a random or an ordered configuration. We find that in both cases the correlation function decays very rapidly and estimate  $\xi_z \approx 1.9$  and  $\xi_z \approx 1.7$  in the LT and HT phase, respectively. Clearly, vector modes are not critical. Similar results hold for the  $\text{CP}^1$  and  $\text{CP}^2$  models. In the first case, we obtain  $\xi_z \approx 2.2$ . For  $N = 3$  the transition is so weak that we cannot identify the two phases and we are only able to compute an effective correlation function, which is a linear combination of those appropriate for the two phases. This quantity still allows us to compute the largest of the two correlation lengths, i.e.,  $\xi_z$  in the LT phase, obtaining  $\xi_z \approx 2.2$ . Results for finite  $\beta_g$  are reported in Fig. 9. The first distinctive feature is that, for the cases we consider, the correlation function does not behave as a single exponential, although an exponential behavior sets when  $x \gg \xi_z$ . Clearly, at the critical point several modes are playing an important role and an exponential behavior is only observed when  $\xi_z$  is significantly less than  $L$ . Second, the correlation length  $\xi_z$  increases with increasing  $\beta_g$  along the transition line. For  $\beta_g = 0.5$  we obtain  $\xi_z \approx 3.8, 3.6, 3.1$  for  $L = 32, 48,$  and  $64$  in the LT phase (runs at  $\beta = 0.370$  with ordered start). In the HT phase (runs at  $\beta = 0.365$ ) we obtain  $\xi_z \approx 2.2$  with a small  $L$  dependence. Although  $\xi_z$  is small, it is larger than the value it takes in the  $\text{CP}^3$  model, i.e. the AH model with  $\beta_g = 0$ . For  $\beta_g = 1$ , we are not able to distinguish the two phases and, therefore, we only compute the LT estimate of  $\xi_z$ . Results for  $L = 32, 48, 64$  essentially agree and give  $\xi_z \approx 6.9$ . This estimate is confirmed by the analysis of the Polyakov loop. A fit to Eq. (35) gives  $\xi_z = 6.9(1)$ , in very good agreement with the results obtained from  $G_V(x)$ . For  $\beta_g = 4$ , even for  $L = 96$  we are not yet in the regime in which one can reliably identify a range of distances in which the correlation function decays exponentially. If we fit the correlation function to Eq. (34) in the range  $L/3 \leq 2L/3$ , we obtain  $\xi_z = 17.1(1)$  and  $17.6(1)$  for  $L = 64$  and  $96$ , respectively. The analysis of the Polyakov loop gives a somewhat larger value  $\xi_z = 20.9(3)$ . Whatever the exact asymptotic result is, data confirm that, for  $\beta_g = 4$ , we are deep in the crossover region, where vector and gauge excitations compete with gauge-invariant excitations associated with  $Q_x$  (for comparison note that  $\xi = 20.3(3)$  for  $L = 96$ ). These results provide us a physical explanation of the crossover effects we observe. The asymptotic first-order behavior is only observed when the correlation length  $\xi(L)$  at the transition point is significantly larger than  $\xi_z$ . When  $\xi(L) \sim \xi_z$  we observe an apparent scaling behavior in which both

the (gauge-field independent) degrees of freedom associated with  $Q$  and the (gauge-field dependent) ones, that are encoded in the gauge observables and in the vector correlations, are both relevant.

#### IV. CONCLUSIONS

We have studied the phase diagram and critical behavior of multicomponent AH lattice models, in which an  $N$ -component complex field  $\mathbf{z}_x$  is coupled to quantum electrodynamics. We consider the compact Wilson formulation of Abelian lattice gauge theories in which the fundamental gauge fields are complex numbers of unit modulus, see Eq. (3). For the scalar fields, we consider the unit-length limit and fix  $|\mathbf{z}_x|^2 = 1$ . Finally, we fix  $q = 1$  for the charge of the matter fields. We focus on systems with a small number of components, considering  $N = 2$  and  $N = 4$ .

We investigate the phase diagram of the model as a function of the couplings  $\beta$  and  $\beta_g$ . The phase diagram is characterized by two phases: a low-temperature phase (large  $\beta$ ) in which the order parameter  $Q^{ab}$  condenses, and a high-temperature disordered phase (small  $\beta$ ). The gauge coupling does not play any particular role in the two phases: gauge observables and vector observables do not show long-range correlations for any finite  $\beta$  and  $\beta_g$ . The two phases are separated by a transition line that connects the  $\text{CP}^{N-1}$  transition point ( $\beta_g = 0$ ) with the  $\text{O}(2N)$  transition point ( $\beta_g = \infty$ ). Concerning the nature of the transition line, our numerical data are consistent with a simple scenario, in which the nature of the transition line is independent of  $\beta_g$ . Therefore, we predict Heisenberg critical behaviors along the whole line for  $N = 2$ , and first-order transitions for  $N = 4$ . Note that, for  $\beta_g \rightarrow \infty$  the model becomes equivalent to the  $\text{O}(2N)$  vector model, and therefore one expects strong crossover effects controlled by the  $\text{O}(2N)$  fixed point. These crossover effects are related to the presence of a second length scale  $\xi_z$  associated with the vector correlations, which is finite for any  $\beta_g$  and diverges in the limit  $\beta_g \rightarrow \infty$  in the whole low-temperature phase.

The scenario supported by our numerical data is fully consistent with the LGW approach that assumes a gauge-invariant order parameter. On the other hand, at least for  $N = 2$ , it disagrees with the  $\varepsilon$ -expansion predictions obtained using the standard continuum AH model: for  $N = 2$  this approach does not predict a continuous transition. Numerical results allow us to understand why the LGW approach is more appropriate than the continuum AH model for these values of  $N$ . At the transition (for both  $N = 2$  and  $N = 4$ ) only correlations of the gauge-invariant operator  $Q^{ab}$  display long-range order. Gauge modes represent a background that gives only rise to crossover effects and indeed, the asymptotic behavior sets in only when the correlation length of the gauge fluctuations is negligible compared to that of the  $Q$  correlations. It is important to note that a LGW ap-

proach based on a gauge-invariant order parameter has also been applied to the study of phase transitions in the presence of nonabelian gauge symmetries, and, in particular, to the study of the finite-temperature transition of hadronic matter as described by the theory of strong interactions, quantum chromodynamics [47–49]. Our results for the AH lattice model lend support to the correctness of the approach and of the predictions obtained.

We expect that AH lattice models with higher (but not too large) values of  $N$  have a phase diagram similar to the one obtained for  $N = 4$ , with a first-order transition line separating the ordered and disordered phases. The phase diagram may change for large values of  $N$ . In this regime, the system may undergo continuous transitions controlled by the stable fixed point of the continuum AH model. This issue requires additional investigations.

It is important to stress that we have considered here a compact version of electrodynamics. Other models of interest in condensed-matter physics consider complex fields (spinons) coupled to noncompact electrodynamics [5, 50, 51]. Such a model may have a different critical behavior due the suppression of monopoles [52–55]. Numerical studies have identified the transition, but at present there is no consensus on its order. The same is true for loop models which supposedly belong to the same universality class (if it exists), see, e.g., Refs. [4, 16, 17, 56, 57]. Clearly, additional work is needed to settle the question.

### Appendix A: Finite-size scaling behavior for $\beta_g \rightarrow \infty$

In this Appendix we discuss the limit  $\beta_g \rightarrow \infty$  of the model. In this limit, the gauge part of the Hamiltonian becomes trivial and we obtain

$$\lambda_{\mathbf{x},\mu} \lambda_{\mathbf{x}+\hat{\mu},\nu} \bar{\lambda}_{\mathbf{x}+\hat{\nu},\mu} \bar{\lambda}_{\mathbf{x},\nu} = 1 \quad (\text{A1})$$

on every lattice plaquette. We consider a finite lattice with periodic boundary conditions and further assume that the Polyakov loops order in the same limit. If this occurs (we discuss this issue in Sec. III D), we can set  $\lambda_{\mathbf{x},\mu} = 1$  on each lattice link. Therefore, for  $\beta_g \rightarrow \infty$ , the Hamiltonian becomes simply

$$H = -\beta N \sum_{\mathbf{x},\mu} (\bar{z}_{\mathbf{x}} \cdot z_{\mathbf{x}+\hat{\mu}} + \text{c.c.}) . \quad (\text{A2})$$

We now define a  $2N$ -dimensional unit real vector  $\mathbf{s}_{\mathbf{x}}$  by setting

$$z_{\mathbf{x}}^a = s_{\mathbf{x}}^a + i s_{\mathbf{x}}^{a+N}, \quad (\text{A3})$$

$a = 1, \dots, N$ . In terms of this new field the Hamiltonian becomes

$$H_V = -n\beta \sum_{\mathbf{x},\mu} \mathbf{s}_{\mathbf{x}} \cdot \mathbf{s}_{\mathbf{x}+\hat{\mu}} \quad (\text{A4})$$

with  $n = 2N$ , which is the Hamiltonian of the  $n$ -vector model. We have therefore an enlargement of the global

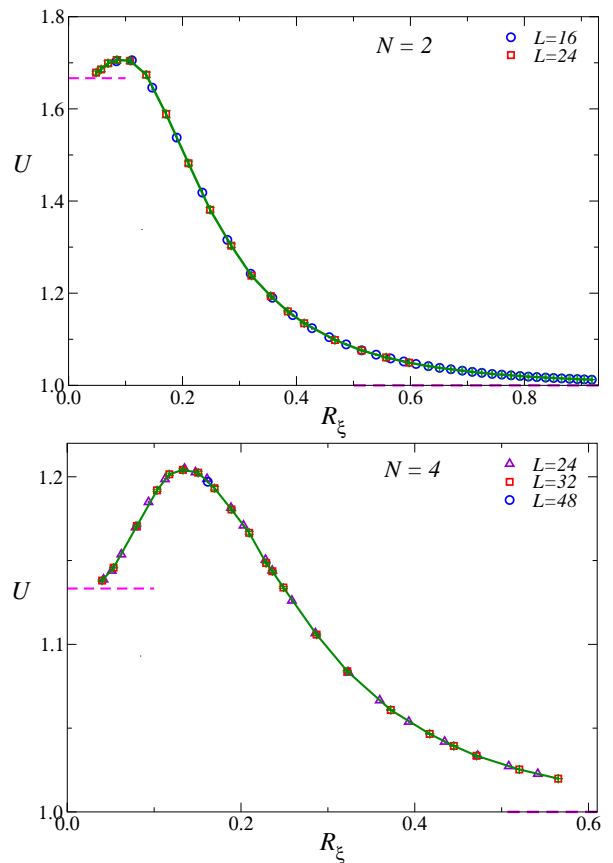


FIG. 10: Scaling functions for the Binder parameter  $U$  versus  $R_\xi \equiv \xi/L$  for  $N = 2$  (top) and  $N = 4$  (bottom), in the large- $\beta_g$  limit, where the model is equivalent to the  $n$ -vector model with  $n = 2N$ . They are obtained by using Eq. (A13) and numerical results for the  $O(4)$  and  $O(8)$  models, respectively. Scaling corrections are tiny: the dashed lines represent a good approximation of the asymptotic FSS curve. The horizontal dashed lines show the asymptotic values  $U(R_\xi \rightarrow 0) = 5/3$  and  $U(R_\xi \rightarrow \infty) = 1$  for  $N = 2$ ,  $U(R_\xi \rightarrow 0) = 17/15$  and  $U(R_\xi \rightarrow \infty) = 1$  for  $N = 4$ .

symmetry: the model is now invariant under  $O(2N)$  transformations.

Since the model becomes  $O(2N)$  invariant, it is useful to rewrite  $CP^{N-1}$  observables in terms of explicitly  $O(2N)$  invariant quantities that can be determined directly in the  $O(2N)$  theory. The basic  $CP^{N-1}$  variable  $Q_{\mathbf{x}}^{ab}$  can be rewritten in terms of the tensor (spin-2) operator of  $O(2N)$  theory:

$$T_{\mathbf{x}}^{\alpha\beta} = s_{\mathbf{x}}^\alpha s_{\mathbf{x}}^\beta - \frac{1}{2N} \delta^{\alpha\beta}, \quad (\text{A5})$$

where  $\alpha, \beta = 1, \dots, 2N$ . The relation is not trivial,

$$Q_{\mathbf{x}}^{ab} = T_{\mathbf{x}}^{ab} + T_{\mathbf{x}}^{a+N, b+N} + iT_{\mathbf{x}}^{a, b+N} - iT_{\mathbf{x}}^{a+N, b}, \quad (\text{A6})$$

which implies that  $Q$ -correlations are not trivially related to  $T$  correlations in the vector model. Using relation (A6), we can express the  $CP^{N-1}$  correlation function

$G(\mathbf{x})$  in terms of the tensor correlation function

$$G_T(\mathbf{x}) = \sum_{\alpha\beta} \langle T_0^{\alpha\beta} T_{\mathbf{x}}^{\alpha\beta} \rangle. \quad (\text{A7})$$

Using the  $O(2N)$  invariance of the model we obtain

$$G(\mathbf{x}) = \frac{2(N-1)}{2N-1} G_T(\mathbf{x}), \quad (\text{A8})$$

which implies that the  $\text{CP}^{N-1}$  correlation length can be identified with the tensor correlation length defined in the  $2N$ -vector model using  $G_T(\mathbf{x})$  and Eq. (17). The Binder parameter  $U$  can also be expressed in terms of analogous quantities defined in the vector model. The relation is more complex and is discussed in detail in the supplementary material [25]. In the  $n$ -vector model we define

$$U_{4T,a} = \frac{\langle \nu_2^2 \rangle}{\langle \nu_2 \rangle^2}, \quad U_{4T,b} = \frac{\langle \nu_4 \rangle}{\langle \nu_2 \rangle^2}, \quad (\text{A9})$$

where

$$\nu_2 = \sum_{\mathbf{x}\mathbf{y}} \text{Tr} T_{\mathbf{x}} T_{\mathbf{y}}, \quad (\text{A10})$$

$$\nu_4 = \sum_{\mathbf{x}\mathbf{y}\mathbf{z}\mathbf{t}} \text{Tr} T_{\mathbf{x}} T_{\mathbf{y}} T_{\mathbf{z}} T_{\mathbf{t}}. \quad (\text{A11})$$

A long calculation gives the relation

$$U = \frac{N(2N-1) [(2N^2 - 5N + 4)U_{4T,a} - 2U_{4T,b}]}{(N-1)^2(2N+1)(2N-3)} \quad (\text{A12})$$

where  $U_{4T,a}$  and  $U_{4T,b}$  are computed in the  $n$ -vector model with  $n = 2N$ . For  $N = 2$  and  $N = 4$ , the two cases of relevance in this work, we obtain:

$$U = \frac{12}{5}(U_{4T,a} - U_{4T,b}),$$

$$U = \frac{448}{405}U_{4T,a} - \frac{56}{405}U_{4T,b}, \quad (\text{A13})$$

respectively. To obtain the scaling functions associated with  $U$  in the large- $\beta_g$  limit for  $N = 2$  and  $4$ , we have therefore performed simulations in the  $n$ -vector model with  $n = 4$  and  $8$ , we have computed the tensor Binder parameters  $U_{4T,a}$  and  $U_{4T,b}$ , and we have applied Eq. (A13). Details on the numerical simulations are reported in the supplementary material [25]. In Fig. 10 we show the resulting curve for  $N = 2$  and  $N = 4$ .

- 
- [1] J. Smiseth, E. Smørgrav, F. S. Nogueira, J. Hove, and A. Sudbø, Phase Structure of  $d = 2 + 1$  Compact Lattice Gauge Theories and the Transition from Mott Insulator to Fractionalized Insulator, *Phys. Rev. B* **67**, 205104 (2003).
- [2] J. Smiseth, E. Smørgrav, and A. Sudbø, Critical properties of the  $N$ -color London model, *Phys. Rev. Lett.* **93**, 077002 (2004).
- [3] E. Babaev, A. Sudbø, and N. W. Ashcroft, A superconductor to superfluid phase transition in liquid metallic hydrogen, *Nature* **431**, 666 (2004).
- [4] O. I. Motrunich and A. Vishwanath, Emergent photons and transitions in the  $O(3)$  sigma model with hedgehog suppression, *Phys. Rev. B* **70**, 075104 (2004).
- [5] T. Senthil, L. Balents, S. Sachdev, A. Vishwanath, and M. P. A. Fisher, Quantum criticality beyond the Landau-Ginzburg-Wilson paradigm, *Phys. Rev. B* **70**, 144407 (2004).
- [6] K. Kataoka, S. Hattori, and I. Ichinose, Effective field theory for  $\text{Sp}(N)$  antiferromagnets and their phase structure, *Phys. Rev. B* **83**, 174449 (2011).
- [7] B.I. Halperin, T.C. Lubensky, and S.K. Ma, First-Order Phase Transitions in Superconductors and Smectic-A Liquid Crystals, *Phys. Rev. Lett.* **32**, 292 (1974).
- [8] M. Moshe and J. Zinn-Justin, Quantum field theory in the large  $N$  limit: A review, *Phys. Rep.* **385**, 69 (2003).
- [9] K. Kajantie, M. Karjalainen, M. Laine, and J. Peisa, Masses and phase structure in the Ginzburg-Landau model, *Phys. Rev. B* **57**, 3011 (1998).
- [10] H. Kleinert, F. S. Nogueira, and A. Sudbø, Deconfinement Transition in Three-Dimensional Compact U(1) Gauge Theories Coupled to Matter Fields, *Phys. Rev. Lett.* **88**, 232001 (2002).
- [11] S. Mo, J. Hove, and A. Sudbø, Order of the metal-to-superconductor transition, *Phys. Rev. B* **65**, 104501 (2002).
- [12] S. Wenzel, E. Bittner, W. Janke, A. M. J. Schakel, and A. Schiller, Kertesz Line in the Three-Dimensional Compact U(1) Lattice Higgs Model, *Phys. Rev. Lett.* **95**, 051601 (2005).
- [13] M. N. Chernodub, E. M. Ilgenfritz, and A. Schiller, Phase structure of an Abelian two-Higgs model and high-temperature superconductors, *Phys. Rev. B* **73**, 100506(R) (2006).
- [14] Note that our coupling  $\beta_g$  differs by a factor of 2 from the one used in other works. If  $\lambda_{\mathbf{x},\mu} = \exp(i\theta_{\mathbf{x},\mu})$ , the gauge part of the Hamiltonian reads  $H_{\text{gauge}} = -2\beta_g \cos \theta_{\mathbf{x},\mu\nu}$ , with  $\theta_{\mathbf{x},\mu\nu} = \theta_{\mathbf{x},\mu} - \theta_{\mathbf{x}+\hat{\nu},\mu} - \theta_{\mathbf{x},\nu} + \theta_{\mathbf{x}+\hat{\mu},\nu}$ .
- [15] A. Pelissetto and E. Vicari, Three-dimensional ferromagnetic  $\text{CP}^{N-1}$  models, *Phys. Rev. E* **100**, 022122 (2019).
- [16] A. Nahum, J. T. Chalker, P. Serna, M. Ortuño, and A. M. Somoza, 3D Loop Models and the  $\text{CP}^{N-1}$  Sigma Model, *Phys. Rev. Lett.* **107**, 110601 (2011).
- [17] A. Nahum, J. T. Chalker, P. Serna, M. Ortuño, and A. M. Somoza, Phase transitions in three-dimensional loop models and the  $\text{CP}^{N-1}$  sigma model, *Phys. Rev. B* **88**, 134411 (2013).
- [18] F. Delfino, A. Pelissetto, and E. Vicari, Three-dimensional antiferromagnetic  $\text{CP}^{N-1}$  models, *Phys. Rev. E* **91**, 052109 (2015).
- [19] A. Pelissetto, A. Tripodo, and E. Vicari, Landau-

- Ginzburg-Wilson approach to critical phenomena in the presence of gauge symmetries, Phys. Rev. D **96**, 034505 (2017).
- [20] A. Pelissetto and E. Vicari, Critical Phenomena and Renormalization Group Theory, Phys. Rep. **368**, 549 (2002).
- [21] T. Ono, S. Doi, Y. Hori, I. Ichinose, and T. Matsui, Phase Structure and Critical Behavior of Multi-Higgs  $U(1)$  Lattice Gauge Theory in Three Dimensions, Ann. Phys. (N.Y.) **324**, 2453 (2009).
- [22] S. Takashima, I. Ichinose, and T. Matsui,  $CP^1+U(1)$  lattice gauge theory in three dimensions: Phase structure, spins, gauge bosons, and instantons, Phys. Rev. B **72**, 075112 (2005).
- [23] In Ref. [6, 21, 22], the system sizes were quite small and the data had a limited precision, preventing the authors to obtain a satisfactory understanding of the nature of the transitions and of the crossover behaviors along the transition lines.
- [24] A. Polyakov, Compact gauge fields and the infrared catastrophe, Phys. Lett. **59B**, 82 (1975); for an extensive list of references, see A. Athenodorou and M. Teper, On the spectrum and string tension of  $U(1)$  lattice gauge theory in  $2+1$  dimensions, J. High Energy Phys. **01**, 063 (2019), and M. Caselle, A. Nada, M. Panero, and D. Vadacchino, Conformal field theory and the hot phase of three-dimensional  $U(1)$  gauge theory, J. High Energy Phys. **05**, 068 (2019).
- [25] In the supplementary material we report results for tensor correlations in  $O(N)$  models and discuss the relation between  $CP^{N-1}$  and  $O(2N)$  Binder parameters for the AH model in the limit  $\beta_g \rightarrow \infty$ .
- [26] B. Ihrig, N. Zerf, P. Marquard, I. F. Herbut, and M. M. Scherer, Abelian Higgs model at four loops, fixed-point collision and deconfined criticality, arXiv:1907.08140.
- [27] R. Folk and Y. Holovatch, On the critical fluctuations in superconductors, J. Phys. A **29**, 3409 (1996).
- [28] L. D. Landau and E. M. Lifshitz, *Statistical Physics. Part I*, 3rd edition (Elsevier Butterworth-Heinemann, Oxford, 1980).
- [29] K. G. Wilson and J. Kogut, The renormalization group and the  $\epsilon$  expansion, Phys. Rep. **12**, 77 (1974).
- [30] M. E. Fisher, The renormalization group in the theory of critical behavior, Rev. Mod. Phys. **47**, 543 (1975).
- [31] S.-k. Ma, *Modern Theory of Critical Phenomena*, (W.A. Benjamin, Reading, MA, 1976).
- [32] A. Pelissetto, A. Tripodo, and E. Vicari, Criticality of  $O(N)$  symmetric models in the presence of discrete gauge symmetries, Phys. Rev. E **97**, 012123 (2018).
- [33] P. Calabrese, P. Parruccini, A. Pelissetto, and E. Vicari, Critical behavior of  $O(2)\otimes O(N)$ -symmetric models, Phys. Rev. B **70**, 174439 (2004).
- [34] Y. Nakayama and T. Ohtsuki, Approaching the conformal window of  $O(n)\times O(m)$  symmetric Landau-Ginzburg models using the conformal bootstrap, Phys. Rev. D **89**, 126009 (2014); Bootstrapping phase transitions in QCD and frustrated spin systems, Phys. Rev. D **91**, 021901 (2015).
- [35] M. De Prato, A. Pelissetto, and E. Vicari, Phys. Rev. B **70**, 214519 (2004).
- [36] M. Campostrini, P. Rossi, and E. Vicari, Monte Carlo simulation of  $CP^{N-1}$  models, Phys. Rev. D **46**, 2647 (1992).
- [37] L. Del Debbio, G. Manca, and E. Vicari, Critical slowing down of topological modes, Phys. Lett. B **594**, 315 (2004).
- [38] M. Hasenbusch, Fighting topological freezing in the two-dimensional  $CP^{N-1}$  model, Phys. Rev. D **96**, 054504 (2017).
- [39] V. Alba, A. Pelissetto, and E. Vicari, The Uniformly Frustrated Two-Dimensional  $XY$  Model in the Limit of Weak Frustration, J. Phys. A: Math. Theor. **41**, 175001 (2008).
- [40] H. G. Ballesteros, L. A. Fernandez, V. Martin-Mayor, A. Munoz Sudupe, Finite size effects on measures of critical exponents in  $d=3$   $O(N)$  models, Phys. Lett. B **387**, 125 (1996).
- [41] M. Campostrini, A. Pelissetto, P. Rossi, E. Vicari, Four-point renormalized coupling in  $O(N)$  models, Nucl. Phys. B **459**, 207 (1996).
- [42] M. Hasenbusch and E. Vicari, Anisotropic perturbations in 3D  $O(N)$  vector models, Phys. Rev. B **84**, 125136 (2011).
- [43] M. Campostrini, M. Hasenbusch, A. Pelissetto, P. Rossi, and E. Vicari, Critical exponents and equation of state of the three-dimensional Heisenberg universality class, Phys. Rev. B **65**, 144520 (2002).
- [44] R. Guida and J. Zinn-Justin, Critical exponents of the  $N$ -vector model, J. Phys. A **31**, 8103 (1998).
- [45] M. S. S. Challa, D. P. Landau, and K. Binder, Finite-size effects at temperature-driven first-order transitions, Phys. Rev. B **34**, 1841 (1986).
- [46] K. Vollmayr, J. D. Reger, M. Scheucher, and K. Binder, Finite size effects at thermally-driven first order phase transitions: A phenomenological theory of the order parameter distribution, Z. Phys. B **91**, 113 (1993).
- [47] R. D. Pisarski and F. Wilczek, Remarks on the chiral phase transition in chromodynamics, Phys. Rev. D **29**, 338 (1984).
- [48] A. Butti, A. Pelissetto, and E. Vicari, On the nature of the finite-temperature transition in QCD, J. High Energy Phys. **08**, 029 (2003).
- [49] A. Pelissetto and E. Vicari, Relevance of the axial anomaly at the finite-temperature chiral transition in QCD, Phys. Rev. D **88**, 105018 (2013).
- [50] T. Senthil, A. Vishwanath, L. Balents, S. Sachdev, and M. P. A. Fisher, Deconfined Quantum Critical Points, Science **303**, 1490 (2004).
- [51] T. Senthil, L. Balents, S. Sachdev, A. Vishwanath, and M. P. A. Fisher, Deconfined Criticality Critically Defined, J. Phys. Soc. Jpn. **74**, 1 (2005).
- [52] M. A. Metliski, M. Harmele, T. Senthil, and M. P. A. Fisher, Monopoles in  $CP^{N-1}$  model via the state-operator correspondence, Phys. Rev. B **78**, 214418 (2008).
- [53] M. S. Block, R. G. Melko, and R. K. Kaul, Fate of  $CP^{N-1}$  Fixed Points with  $q$  Monopoles, Phys. Rev. Lett. **111**, 137202 (2013).
- [54] G. J. Sreejith and S. Powell, Scaling dimensions of higher-charge monopoles at deconfined critical points, Phys. Rev. B **92**, 184413 (2015).
- [55] E. Dyer, M. Mezei, S. S. Pufu, and S. Sachdev, Scaling dimensions of monopole operators in the  $CP^{N_b-1}$  theory in  $2+1$  dimensions, J. High Energy Phys. **06**, 037 (2015).
- [56] A. B. Kuklov, M. Matsumoto, N. V. Prokofiev, B. V. Svistunov, and M. Troyer, Deconfined Criticality: Generic First-Order Transition in the  $SU(2)$  Symmetry Case, Phys. Rev. Lett. **101**, 050405 (2008).
- [57] A. Nahum, J. T. Chalker, P. Serna, M. Ortuño, and A. M. Somoza, Deconfined Quantum Criticality, Scaling Viola-

tions, and Classical Loop Models, Phys. Rev. X **5**, 041048 (2015).

# Supplementary material for “Multicomponent compact Abelian-Higgs lattice models”

---

## 1. Scaling functions in the $N$ vector model

We consider the three-dimensional  $N$ -vector model on a cubic lattice. We define an  $N$ -dimensional real spin vector  $s_{\mathbf{x}}^{\alpha}$  on each lattice site and consider the Hamiltonian

$$\mathcal{H} = - \sum_{\langle \mathbf{x} \mathbf{y} \rangle} \mathbf{s}_{\mathbf{x}} \cdot \mathbf{s}_{\mathbf{y}}. \quad (\text{A14})$$

The sum in Eq. (A14) extends over all lattice nearest-neighbor pairs  $\langle \mathbf{x} \mathbf{y} \rangle$ . In this supplementary material we investigate the critical behavior of tensor observables, defined in terms of the tensor (matrix) field

$$T_{\mathbf{x}}^{\alpha\beta} = s_{\mathbf{x}}^{\alpha} s_{\mathbf{x}}^{\beta} - \frac{1}{N} \delta^{\alpha\beta}. \quad (\text{A15})$$

We define the tensor correlation function

$$G_T(\mathbf{x}) = \sum_{\alpha\beta} \langle T_{\mathbf{0}}^{\alpha\beta} T_{\mathbf{x}}^{\alpha\beta} \rangle = \langle \text{Tr} (T_{\mathbf{0}} T_{\mathbf{x}}) \rangle, \quad (\text{A16})$$

where “Tr” is the trace over the  $O(N)$  indices, and the corresponding correlation length

$$\xi_T^2 = \frac{1}{4 \sin^2(\pi/L)} \frac{\tilde{G}_T(\mathbf{0}) - \tilde{G}_T(\mathbf{p}_m)}{\tilde{G}_T(\mathbf{p}_m)}. \quad (\text{A17})$$

Here  $\tilde{G}_T(\mathbf{p}) = \sum_{\mathbf{x}} G_T(\mathbf{x}) e^{i\mathbf{p}\cdot\mathbf{x}}$  and  $\mathbf{p}_m = (2\pi/L, 0, 0)$ . Definitions (A16) and (A17) are the obvious generalizations of those used for spin-spin correlations. In this case one considers the vector correlation function

$$G_V(\mathbf{x}) = \langle \mathbf{s}_{\mathbf{0}} \cdot \mathbf{s}_{\mathbf{x}} \rangle, \quad (\text{A18})$$

and the vector correlation length  $\xi_V$  defined using Eq. (A17) and  $G_V(\mathbf{x})$ .

Beside the correlation length, we also consider renormalization-group invariant ratios (collectively named Binder parameters) defined in terms of

$$\Theta^{\alpha\beta} = \sum_{\mathbf{x}} T_{\mathbf{x}}^{\alpha\beta}. \quad (\text{A19})$$

We define

$$U_{3T} = \frac{\langle \text{Tr} \Theta^3 \rangle}{\langle \text{Tr} \Theta^2 \rangle^{3/2}}, \quad (\text{A20})$$

$$U_{4T,a} = \frac{\langle [\text{Tr} \Theta^2]^2 \rangle}{\langle \text{Tr} \Theta^2 \rangle^2} \quad U_{4T,b} = \frac{\langle \text{Tr} \Theta^4 \rangle}{\langle \text{Tr} \Theta^2 \rangle^2}. \quad (\text{A21})$$

These quantities are not independent for  $N = 2$  and  $3$ . The relation  $U_{4T,b} = U_{4T,a}/2$  holds for  $N = 2, 3$ , while  $U_3 = 0$  for  $N = 2$ .

TABLE I: Estimates of the Binder parameters in the high-temperature (HT) and low-temperature (LT) phase.  $U_{3T} = 0$  in the HT phase.

$N$	HT		LT		
	$U_{4T,a}$	$U_{4T,b}$	$U_{3T}$	$U_{4T,a}$	$U_{4T,b}$
3	1.400	0.700	0.408	1	0.500
4	1.222	0.528	0.577	1	0.583
5	1.143	0.421	0.671	1	0.650
8	1.057	0.261	0.802	1	0.768
$\infty$	1	0	1	1	1

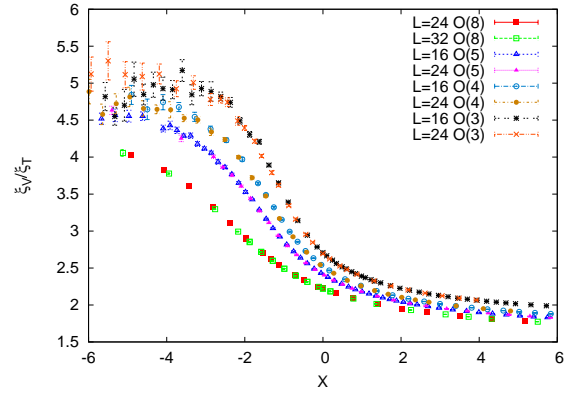


FIG. 11: Plot of  $\xi_V/\xi_T$  as a function of  $X = (\beta - \beta_c)L^{1/\nu}$  for  $N = 3, 4, 5$  and  $8$ .

We can easily predict the value the Binder parameters take in the high-temperature phase. The cubic parameter  $U_{3T}$  vanishes, while

$$U_{4T,a} = \frac{N^2 + N + 2}{(N+2)(N-1)} \quad U_{4T,b} = \frac{2N^2 + 3N - 6}{N(N+2)(N-1)}. \quad (\text{A22})$$

In the low-temperature phase we obtain instead

$$U_{3T} = \frac{N-2}{\sqrt{N(N-1)}}, \quad (\text{A23})$$

$$U_{4T,a} = 1 \quad U_{4T,b} = \frac{N^2 - 3N + 3}{N(N-1)}. \quad (\text{A24})$$

Numerical results for  $N = 3, 4, 5, 8$  are reported in Table I.

Close to the critical point, for  $L \rightarrow \infty$ , renormalization-group invariant quantities  $R$  satisfy the scaling law

$$R(\beta, L) = f_R(X) + O(L^{-\omega}) \quad X = (\beta - \beta_c)L^{1/\nu}. \quad (\text{A25})$$

TABLE II: Estimates of several renormalization-group invariant quantities at the critical point  $X = 0$ .

	$N = 3$	$N = 4$	$N = 5$	$N = 8$
$U_{4T,a}^*$	1.458(12)	1.287(7)	1.218(2)	1.117(2)
$U_{4T,b}^*$	0.729(6)	0.684(2)	0.677(3)	0.681(2)
$U_{3T}^*$	0.334(10)	0.462(7)	0.529(3)	0.636(2)
$(\xi_T/L)^*$	0.213(5)	0.221(4)	0.222(1)	0.236(1)
$(\xi_V/\xi_T)^*$	2.68(3)	2.50(2)	2.41(1)	2.21(1)

Here  $\beta_c$  is the critical-point position,  $\nu$  the correlation-length exponent and  $\omega$  is the exponent that controls scaling corrections (in  $N$  vector models it varies between 0.8 and 1, see Ref. [1]). The function  $f_R(X)$  is universal apart from a rescaling of its argument. In particular, its value  $R^* = f_R(0)$  at the critical point is universal. As we have done in the paper, we can also parametrize the scaling behavior by using a specific quantity  $R$ . Here we use the ratio  $R_{\xi,T} = \xi_T/L$ , rewriting Eq. (A25) as

$$R(\beta, L) = g_R(\xi_T/L) + O(L^{-\omega}). \quad (\text{A26})$$

The function  $g_R(x)$  is universal.

We have computed several scaling functions for  $N = 3, 4, 5, 8$  on cubic lattices of size  $L$ , with  $L$  in the interval  $16 \leq L \leq 32$ . We use periodic boundary conditions. In Figs. 11 and 12 we report the scaling functions as a function of  $X$ . We have used the following values for  $\beta_c$  and  $\nu$ :  $\beta_c = 0.69302(3)$  [3, 5] and  $\nu = 0.7112(5)$  [4] for  $N = 3$ ;  $\beta_c = 0.93586(1)$  [5, 6] and  $\nu = 0.749(2)$  [7] for  $N = 4$ ;  $\beta_c = 1.18138(3)$  and  $\nu = 0.779(3)$  [8] for  $N = 5$ ;  $\beta_c = 1.92677(2)$  and  $\nu = 0.85(2)$  [9] for  $N = 8$ . Note that, on the scale of the figure, differences on the value of  $\nu$  of 1% cannot be distinguished.

In spite of the fact that lattices are relatively small, we observe a very good scaling. We have also determined the value of the different quantities at the critical point, see Table II. The results have been obtained by extrapolating the finite- $L$  data assuming that scaling corrections behave as  $L^{-\omega}$ . The quoted error includes the statistical error, the interpolation error of the data, the error on  $\beta_c$  and  $\nu$ , and the extrapolation error. The latter has been conservatively estimated as the difference between the extrapolated value and the value that the observable takes on the largest lattice.

In Fig. 13 we report the same invariant ratios as a function of  $\xi_T/L$ . Some numerical values (extrapolations and errors have been computed as before) are reported in Table A 1.

## 2. $\text{CP}^{N-1}$ Binder parameters in the $\text{O}(2N)$ theory

In the limit  $\beta_g \rightarrow \infty$ , the gauge field  $\lambda_{\mathbf{x},\mu}$  can be set equal to one and the model reduces to a vector model with a  $2N$  dimensional real spin field. We wish now to compute the limiting behavior of the scaling functions for

the  $\text{CP}^{N-1}$  Binder parameters. As we have done for the  $N$ -vector theory, we define three Binder parameters. If

$$Q_{\mathbf{x}}^{ab} = \bar{z}_{\mathbf{x}}^a \bar{z}_{\mathbf{x}}^b - \frac{1}{N} \delta^{ab} \quad \Theta_{CP}^{ab} = \sum_{\mathbf{x}} Q_{\mathbf{x}}^{ab}, \quad (\text{A27})$$

we define

$$U_{3CP} = \frac{\langle \text{Tr } \Theta_{CP}^3 \rangle}{\langle \text{Tr } \Theta_{CP}^2 \rangle^{3/2}}, \quad (\text{A28})$$

$$U_{4CP,a} = \frac{\langle [\text{Tr } \Theta_{CP}^2]^2 \rangle}{\langle \text{Tr } \Theta_{CP}^2 \rangle^2} \quad U_{4CP,b} = \frac{\langle \text{Tr } \Theta_{CP}^4 \rangle}{\langle \text{Tr } \Theta_{CP}^2 \rangle^2}. \quad (\text{A29})$$

The quantity named here  $U_{4CP,a}$  is the Binder parameter  $U_4$  presented in the main text. For  $N = 2$ , we have  $U_{3CP} = 0$  and  $U_{4CP,a} = 2U_{4CP,b}$ .

In the high-temperature phase we have  $U_{3CP} = 0$ ,

$$U_{4CP,a} = \frac{N^2 + 1}{N^2 - 1} \quad U_{4CP,b} = \frac{2N^2 - 3}{N(N^2 - 1)}. \quad (\text{A30})$$

In the low-temperature phase we have  $U_{4CP,a} = 1$ ,

$$U_{3CP} = \frac{N - 2}{\sqrt{N(N - 1)}}, \quad (\text{A31})$$

$$U_{4CP,b} = \frac{N^2 - 3N + 3}{N(N - 1)}. \quad (\text{A32})$$

To compute the scaling functions associated with these quantities in the  $\text{O}(2N)$  theory, we use the mapping

$$z_{\mathbf{x}}^a = s_{\mathbf{x}}^a + i s_{\mathbf{x}}^{a+N}, \quad (\text{A33})$$

where  $1 \leq a \leq N$  and  $s_{\mathbf{x}}^a$  is a  $2N$ -dimensional real unit vector. It is then easy to verify that

$$\Theta_{CP}^{ab} = \Theta^{ab} + \Theta^{a+N,b+N} + i\Theta^{a,b+N} - i\Theta^{a+N,b}, \quad (\text{A34})$$

where  $\Theta^{ab}$  is the  $2N$ -dimensional real quantity defined in Eq. (A19). Squaring the previous relation and taking the trace, we obtain

$$\text{Tr } \Theta_{CP}^2 = \text{Tr } \Theta^2 + \sum_{a,b=1}^N (\Theta^{ab} \Theta^{a+N,b+N} - \Theta^{a,b+N} \Theta^{a+N,b}). \quad (\text{A35})$$

In this relation, the trace in the l.h.s. is performed in the  $\text{CP}^{N-1}$  theory (indices go from 1 to  $N$ ), while the trace in the r.h.s. is performed in the  $\text{O}(2N)$  theory (indices go from 1 to  $2N$ ). The presence of the additional terms in Eq. (A35) explains why the relation between the  $\text{CP}^{N-1}$  Binder parameters and the tensor Binder parameters in the  $\text{O}(2N)$  theory is not trivial.

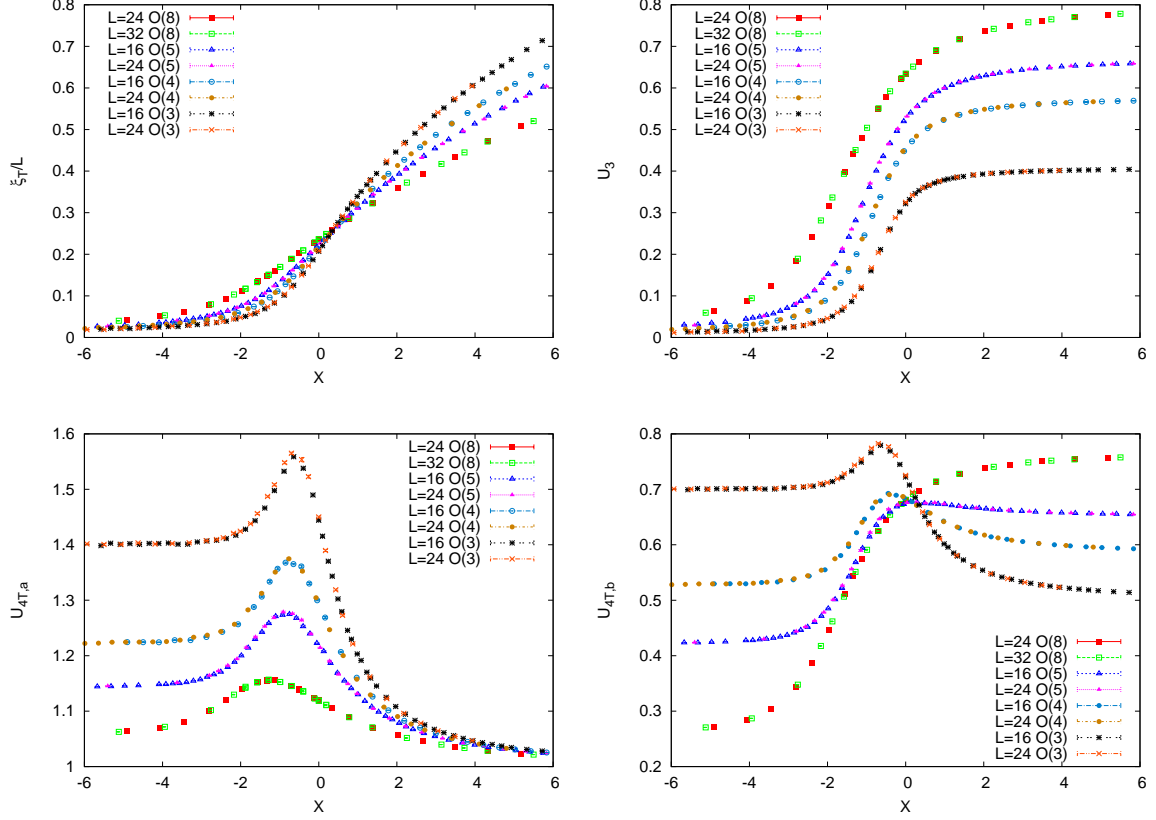


FIG. 12: Plot of  $\xi_T/L$  (top left),  $U_{3T}$  (top right),  $U_{4T,a}$  (bottom left), and  $U_{4T,b}$  (top right) as a function of  $X = (\beta - \beta_c)L^{1/\nu}$  for  $N = 3, 4, 5$  and  $8$ .

Using the  $O(2N)$  invariance of the model we obtain the relations

$$\begin{aligned}
 \langle \text{Tr } \Theta_{CP}^2 \rangle &= \frac{2(N-1)}{2N-1} \langle \text{Tr } \Theta^2 \rangle, \\
 \langle \text{Tr } \Theta_{CP}^3 \rangle &= \frac{2(N-2)}{2N-1} \langle \text{Tr } \Theta^3 \rangle, \\
 \langle [\text{Tr } \Theta_{CP}^2]^2 \rangle &= \frac{4N}{(2N-3)(4N^2-1)} \times \\
 &\quad \times [(2N^2-5N+4)\langle [\text{Tr } \Theta^2]^2 \rangle - 2\langle \text{Tr } \Theta^4 \rangle], \\
 \langle \text{Tr } \Theta_{CP}^4 \rangle &= \frac{2}{(2N-3)(4N^2-1)} \times \\
 &\quad \times [(4N^2-3N-6)\langle [\text{Tr } \Theta^2]^2 \rangle + \\
 &\quad + 2(2N^3-9N^2+6N+6)\langle \text{Tr } \Theta^4 \rangle]. \tag{A36}
 \end{aligned}$$

We obtain therefore the relations, which are exact for the  $O(2N)$  theory, between  $CP^{N-1}$  and tensor  $O(2N)$  Binder

parameters:

$$\begin{aligned}
 U_{3CP} &= \frac{N-2}{N-1} \sqrt{\frac{2N-1}{2(N-1)}} U_{3T}, \\
 U_{4CP,a} &= \frac{N(2N-1)}{(N-1)^2(2N+1)(2N-3)} \times \\
 &\quad \times [(2N^2-5N+4)U_{4T,a} - 2U_{4T,b}], \\
 U_{4b,CP} &= \frac{2N-1}{2(N-1)^2(2N+1)(2N-3)} \times \\
 &\quad \times [(4N^2-3N-6)U_{4T,a} + \\
 &\quad + 2(2N^3-9N^2+6N+6)U_{4T,b}]. \tag{A37}
 \end{aligned}$$

For the  $CP^1$  model ( $N = 2$ ) the only independent Binder parameter  $U_{4CP,a}$  is related to the tensor Binder parameters in the  $O(4)$  theory by

$$U_{4CP,a} = \frac{12}{5}(U_{4T,a} - U_{4T,b}). \tag{A38}$$

For the  $CP^3$  model ( $N = 4$ ) the relation between  $CP^3$

TABLE III: We report some numerical values for the scaling function  $g_R(x)$  ( $x = \xi_T/L$ ) defined in Eq. (A26) for  $N = 3, 4, 5, 8$ . If the function has a maximum, in the second column we report the position  $x_{\max}$  of the maximum and  $\text{Max} = g_R(x_{\max})$ . In the last five columns we report  $g_R(x)$  for  $x = 0.1, 0.2, 0.3, 0.4, 0.5$ .

$N$	$x_{\max}$	Max	$x = 0.1$	$x = 0.2$	$x = 0.3$	$x = 0.4$	$x = 0.5$
$U_{3T}$							
3			0.162(4)	0.325(8)	0.372(2)	0.390(2)	0.398(1)
4			0.212(1)	0.422(8)	0.517(2)	0.548(2)	0.561(1)
5			0.246(7)	0.502(7)	0.597(3)	0.634(2)	0.654(1)
8			0.268(1)	0.576(3)	0.703(2)	0.753(1)	0.775(1)
$U_{4T,a}$							
3	0.132(2)	1.60(3)	1.57(3)	1.49(2)	1.261(2)	1.146(5)	1.080(1)
4	0.141(2)	1.39(2)	1.336(5)	1.317(2)	1.178(4)	1.099(2)	1.054(1)
5	0.155(1)	1.29(1)	1.250(7)	1.256(2)	1.144(4)	1.075(2)	1.041(1)
8	0.154(1)	1.17(1)	1.1269(3)	1.142(2)	1.089(3)	1.044(1)	1.0239(4)
$U_{4T,b}$							
3	0.132(2)	0.80(2)	0.78(2)	0.745(1)	0.631(1)	0.573(2)	0.540(1)
4	0.205(1)	0.692(6)	0.626(3)	0.685(3)	0.649(2)	0.622(2)	0.604(1)
5	0.25(4)	0.68(1)	0.549(7)	0.679(9)	0.678(4)	0.665(2)	0.658(1)
8			0.407(1)	0.644(3)	0.721(2)	0.746(1)	0.7562(2)
$\xi_V/\xi_T$							
3			3.37(5)	2.71(2)	2.46(1)	2.296(8)	2.171(8)
4			3.23(5)	2.62(3)	2.30(1)	2.125(4)	2.008(7)
5			3.18(2)	2.49(2)	2.20(1)	2.029(3)	1.918(6)
8			3.01(2)	2.34(1)	2.05(1)	1.893(3)	1.788(4)

and O(8) Binder parameters is

$$\begin{aligned}
 U_{3CP} &= \sqrt{\frac{14}{27}} U_{3T}, \\
 U_{4CP,a} &= \frac{448}{405} U_{4T,a} - \frac{56}{405} U_{4T,b}, \\
 U_{4CP,b} &= \frac{161}{405} U_{4T,a} + \frac{98}{405} U_{4T,b}. \quad (\text{A39})
 \end{aligned}$$

For the comparison it is also important to relate the correlation length. In the  $\text{CP}^{N-1}$  it is defined from the correlation function of  $Q_x$ :

$$G_{CP}(\mathbf{x}) = \langle \text{Tr} Q_0 Q_{\mathbf{x}} \rangle. \quad (\text{A40})$$

In the O(2N) theory, we have the relation

$$G_{CP}(\mathbf{x}) = \frac{2(N-1)}{2N-1} G_T(\mathbf{x}), \quad (\text{A41})$$

As the correlation length does not depend on the normalization of the correlation function, the correlation length  $\xi_{CP}$  computed from  $G_{CP}(\mathbf{x})$  is identical to the O(2N) tensor correlation length  $\xi_T$ . The scaling functions for the  $\text{CP}^{N-1}$  Binder parameters  $U_{4CP,a}$  and  $U_{4CP,b}$  are reported in Fig. 14 for  $N = 2$  and 4.

---

### References for the supplementary material

- [1] A. Pelissetto and E. Vicari, Critical Phenomena and Renormalization Group Theory, Phys. Rep. **368**, 549 (2002).
- [2] H. G. Ballesteros, L. A. Fernández, V. Martín-Mayor, A. Muñoz-Sudupe, Finite size effects on measures of critical exponents in  $d = 3$  O(N) models, Phys. Lett. **387**, 125 (1996).
- [3] P. Butera and M. Comi,  $N$ -vector spin models on the simple-cubic and the body-centered-cubic lattices: A study of the critical behavior of the susceptibility and of the correlation length by high-temperature series extended to order  $\beta^{21}$ , Phys. Rev. B **56**, 8212 (1997).
- [4] M. Campostrini, M. Hasenbusch, A. Pelissetto, P. Rossi, and E. Vicari, Critical exponents and equation of state of the three-dimensional Heisenberg universality class, Phys. Rev. B **65**, 144520 (2002).

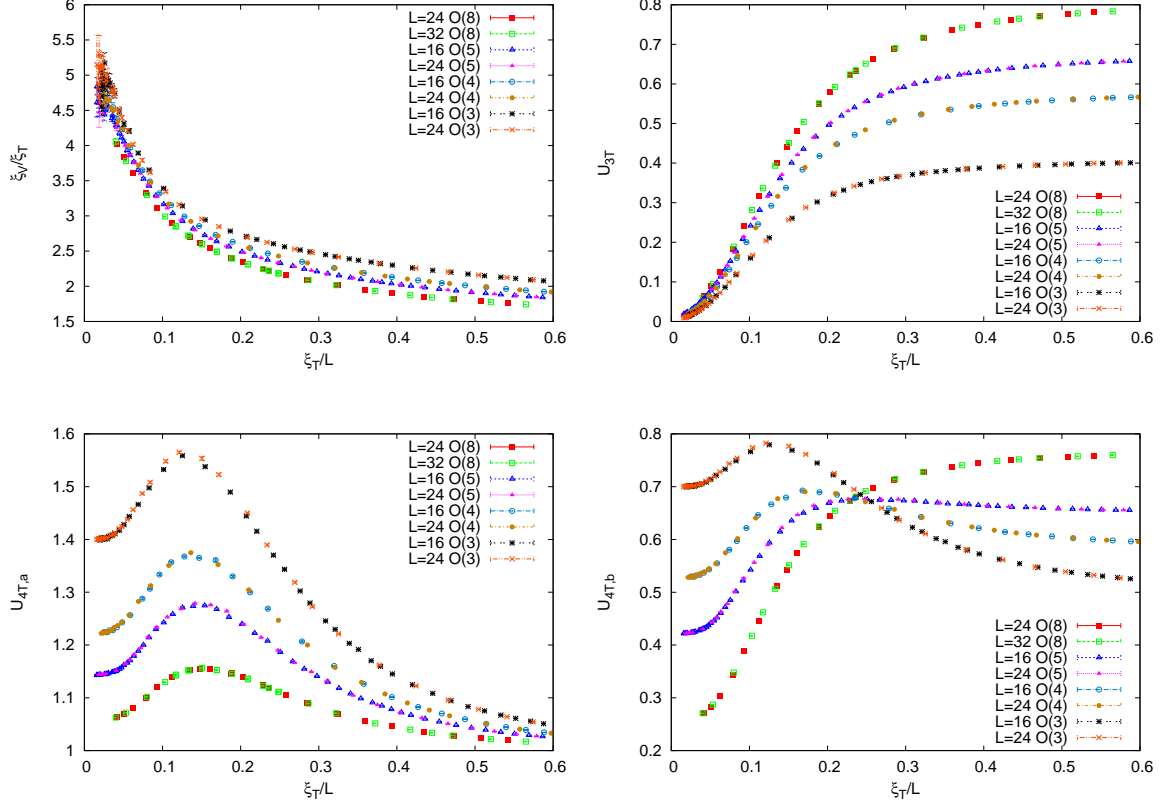


FIG. 13: Plot of  $\xi_V/\xi_T$  (top left),  $U_{3T}$  (top right),  $U_{4T,a}$  (bottom left), and  $U_{4T,b}$  (top right) as a function of  $\xi_T/L$  for  $N = 3, 4, 5$  and  $8$ .

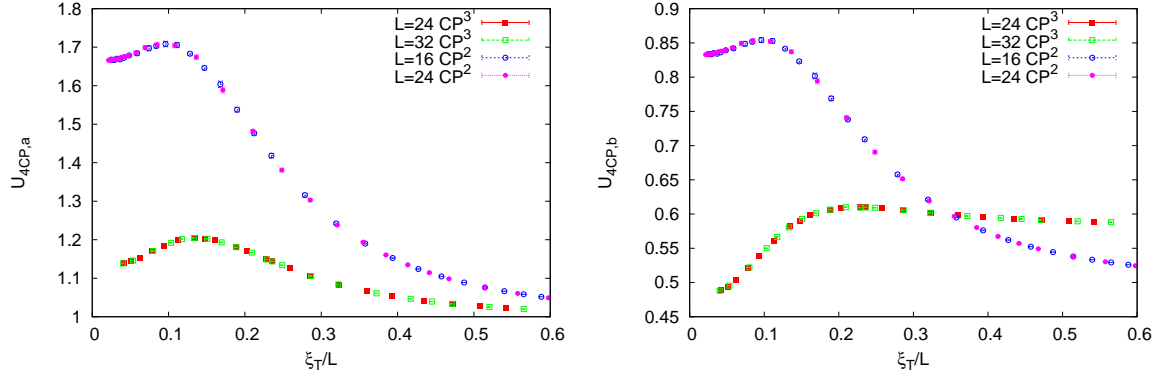


FIG. 14: Scaling functions of the  $CP^{N-1}$  Binder parameters in the  $O(2N)$  model, computed using  $O(2N)$  tensor data and Eq. (A37). For  $N = 2$  we have  $U_{4CP,b} = U_{4CP,a}/2$ . For  $\xi_T/L \rightarrow 0$ , we have  $U_{4CP,a} \approx 1.667$ ,  $U_{4CP,b} \approx 0.833$  for  $N = 2$  and  $U_{4CP,a} \approx 1.133$ ,  $U_{4CP,b} \approx 0.483$  for  $N = 4$ . In the limit  $\xi_T/L \rightarrow \infty$ ,  $U_{4CP,a} = 1$  and  $U_{4CP,b} = 0.5, 0.583$  for  $N = 2, 4$ , respectively.

- [5] H. G. Ballesteros, L. A. Fernandez, V. Martin-Mayor, A. Munoz Sudupe, Finite size effects on measures of critical exponents in  $d = 3$   $O(N)$  models, Phys. Lett. B **387**, 125 (1996).
- [6] M. Campostrini, A. Pelissetto, P. Rossi, E. Vicari, Four-point renormalized coupling in  $O(N)$  models, Nucl. Phys. B **459**, 207 (1996).
- [7] M. Hasenbusch, Eliminating leading corrections to scaling in the three-dimensional  $O(N)$ -symmetric  $\phi^4$  model:  $N = 3$  and  $4$ , J. Phys. A **34**, 8221 (2001).

- [8] M. Hasenbusch, A. Pelissetto, and E. Vicari, Instability of  $O(5)$  multicritical behavior in  $SO(5)$  theory of high- $T_c$  superconductors, *Phys. Rev. B* **72**, 014532 (2005).
  - [9] F. Delfino, A. Pelissetto, and E. Vicari, Three-dimensional antiferromagnetic  $CP^{N-1}$  models, *Phys. Rev. E* **91**, 052109 (2015).
-